Daryna Piontkivska

Bachelor degree in Biochemistry

Unravelling how the biosynthesis of sphingolipids impacts stress responses in *Aspergillus nidulans*

Dissertation to obtain the Master Degree in Biochemistry for Health

Supervisor: Cristina Silva Pereira, PI, ITQB-NOVA

Co-supervisor: Diego de Oliveira Hartmann, PhD, ITQB-NOVA

September 2017

Daryna Piontkivska

Bachelor degree in Biochemistry

Unravelling how the biosynthesis of sphingolipids impacts stress responses in *Aspergillus nidulans*

Dissertation to obtain the Master Degree in Biochemistry for Health

Supervisor: Cristina Silva Pereira, PI, ITQB-NOVA

Co-supervisor: Diego de Oliveira Hartmann, PhD, ITQB-NOVA

Members of the jury:

President: Dr. Pedro Matias, ITQB/UNL

Thesis Examiner: Dr. Catarina Pimentel, ITQB/UNL

Thesis Supervisor: Dr. Cristina Silva Pereira, ITQB/UNL

Instituto de Tecnologia Química e Bioquímica António Xavier, Oeiras

September 2017

Título: Unravelling how the biosynthesis of sphingolipids impacts stress responses in *Aspergillus nidulans*

Daryna Piontkivska acknowledges funding through the fellowship (024/BI/2017) granted within the project funded by the European Research Council through grant ERC-2014-CoG-647928 coordinated by Professor Cristina Silva Pereira. The work was also partially funded by Fundação para a Ciência e Tecnologia through grant UID/Multi/04551/2013 (Research unit GREEN-it "Bioresources for Sustainability").

Acknowledgments

The completion of this dissertation was only possible with the support of many to whom I wish to thank.

Working in the Applied and Environmental Mycology was both an honour and a pleasure. I would like to express my gratitude to Dr. Cristina Silva Pereira, my supervisor, for giving me the opportunity to work in her lab and especially for helping me, encouraging me to move forward and for believing in my potential.

I would also to thank Diego Hartmann, my co-supervisor, for supporting my thesis and for the suggestions given. To all members of AEM lab for always providing a good working environment and sharing a good mood, for the jokes and strength to overcome the hard times. I wish to thank Rúben for his patience and for helping and motivating me. Also, I would like to give thanks to Patrícia Sequeira for sharing this adventure and experience with me, and a special thanks to Patrícia Gonçalves, Maika, Vanessa, Adélia, Isabel, Carlos, Celso and Joana.

To the friends I have made during my academic years for always being by my side and whose concern and strength has helped me to evolve in every aspects of my being. Therefore, Andreia, Diana and Filipa, and many others, a sincere thank you. To my best friend Sofia for all the talks and unconditional support.

I cannot end without thanking to my parents for always supporting and guiding me so I could follow my heart.

Resumo

Nos últimos anos, fungos filamentosos emergiram como agentes patogénicos provocando cada vez mais infeções mortais. Os antifúngicos atualmente disponíveis são inadequados para combater esta crescente ameaça global, assim sendo a descoberta de novos alvos antifúngicos é de extrema importância. Neste contexto, os esfingolipídos surgiram como potenciais alvos para o desenvolvimento de novos agentes antifúngicos. Apesar disso, o conhecimento das vias biossintéticas de esfingolipídos em fungos filamentosos, como *Aspergillus nidulans*, é bastante limitado. Estudos anteriores sugerem que alguns líquidos iónicos desencadeiam a acumulação de intermediários esfingolipídicos que possivelmente desempenham a função de mensageiros secundários em resposta ao stress. Neste estudo, o principal objetivo consistiu em avaliar como a biossíntese de esfingolipídos afeta a resposta de A. *nidulans* ao stress imposto. Desta forma, foram identificados cinco genes possivelmente envolvidos nas modificações estruturais dos esfingolipídos em *A. nidulans* e estirpes com a deleção de cada um dos genes foram produzidas. O perfil de acumulação de bases esfingóides de cada um dos mutantes foi inicialmente caracterizado através da utilização de cromatografia líquida, bem como as suas respostas aos líquidos iónicos $[C_{10}mim]Cl$, $[P_{4\,4\,4\,12}]Cl$ ou decanoato de colina. Para complementar estas análises, foi também avaliada a suscetibilidade das estirpes mutantes aos líquidos iónicos testados. Estas estirpes parecem responder de maneiras distintas e mostram diferentes suscetibilidades para cada um dos líquidos iónicos testados. Foi realizada também uma análise preliminar da influência dos esfingolípidos na resposta aos agentes antifúngicos itraconazol, fluconazol, anfotericina B, flucitosina e terbinafina. As estirpes mutantes em estudo mostraram diferentes características de suscetibilidade ou resistência aos diferentes fármacos testados. O conjunto de dados apresentados reforça o significado da via biossintética de esfingolipídos em resposta ao stress. Compreender a relação entre a resposta desta via e o modo de ação de líquidos iónicos e agentes antifúngicos parece ser bastante promissor.

Palavras-chave: *Aspergillus nidulans*, esfingolipídos, líquidos iónicos, agentes antifúngicos

Abstract

For the past years filamentous fungi have been emerging as critical human-pathogens and have been increasingly provoking deadly invasive infections. The currently available antifungal drugs are inadequate to fight this global threat and the discovery of new antifungal targets are urgently needed. In this context, fungal sphingolipids have come up as potential targets for the development of new antifungal agents; however, knowledge on sphingolipid biosynthetic pathways in filamentous fungi, such as *Aspergillus nidulans,* is still rather limited. Previous observations demonstrated that some ionic liquids can trigger the accumulation of sphingolipid intermediates of the glucosylceramide biosynthetic pathway, that in response to the induced stress are probably acting as second messengers. In the present thesis we wanted to assess how sphingolipid biosynthesis can impact stress responses in *A. nidulans*. Five putative genes involved in the glucosylceramide pathway in *A. nidulans* were identified and deletion strains for each one were generated. The diversity of sphingoid bases accumulation of each mutant was initially characterised by liquid chromatography, as well as their response to the ionic liquids $[C_{10}mim]Cl$, $[P_{4\,4\,4\,12}]Cl$ or cholinium decanoate. To complement these analyses, the susceptibility of the mutant strains to the tested ionic liquids was also assessed. The deleted strains apparently responded in distinct manners and displayed different susceptibilities to each ionic liquid. Ultimately, a preliminary analysis of sphingolipids influence in the fungal response to the known antifungal drugs itraconazole, fluconazole, amphotericin B, flucytosine and terbinafine was performed. The mutants showed distinct susceptibility or resistance profiles to the different antifungal drugs. Overall, the initial datasets herein presented reinforce the significance of the sphingolipid pathway in stress responses; Understanding the relation between the glucosylceramide pathway response and the mode of action of either ionic liquids or conventional antifungal drugs in filamentous fungi, surely merits further research.

Keywords: *Aspergillus nidulans*, glucosylceramide pathway, sphingolipids, ionic liquids, antifungal drugs

General Index

Acknowledgments i

Resumo iii

Abstract v

General Index vii

Figure Index ix

Table Index xi

List of Acronyms xiii

CHAPTER 1 – Introduction 1

1.1 The Fungal Kingdom 2

1.2 Fungal Taxonomy 3

1.3 *Aspergillus nidulans* 5

1.4 Antifungal Drugs 6

1.5 Sphingolipid Biosynthesis 8

1.6 Ionic Liquids 10

1.7 Objectives 12

CHAPTER 2 – Materials and Methods 13

2.1 Chemicals 14

2.2 Strains and storage conditions 15

2.3 Culture mediums 15

2.4 Generation of deletion strains 16

2.4.1 Construction of deletion cassettes 16

2.4.2 Generation of transformable protoplasts and their transformation 19

2.4.3 Selection and confirmation 20

2.5 Determination of minimal inhibitory concentrations of ionic liquids 20

2.6 Determination of radial growth in solid medium supplemented with ionic liquids 21

2.7 Lipid content assessment 21

2.8 High performance liquid chromatography analysis....22
2.9 Determination of susceptibility to antifungal drugs....22
CHAPTER 3 – Results....25
3.1 Gene identification for target deletion....26
3.2 Confirmation of gene deletion....27
3.3 Sphingoid bases chromatographic profile of mutant strains....30
3.4 Ionic liquids minimal inhibitory concentration....32
3.5 Growth ability in presence of ionic liquids....32
3.6 Analysis of sphingoid base accumulation induced by ionic liquids....35
3.7 Susceptibility to antifungal drugs....38
CHAPTER 4 – Discussion and Future Perspectives....41
CHAPTER 5 – Conclusion....51
REFERENCES....53

Figure Index

Figure 1.1. Phylogeny and classification of the Kingdom Fungi, according to Hibbett *et al*. (23). Branch lengths are not proportional to genetic distances…… **4**

Figure 1.2. Schematic representation of *Aspergillus nidulans* life cycle adapted from (38). The sexual, asexual and parasexual cell cycles are indicated by the purple, orange and green arrows, respectively……..... **6**

Figure 1.3. Structure of representative examples of antifungal drugs in current clinical use, adapted from (44)…… **7**

Figure 1.4. Overview of the sphingolipid biosynthetic pathways in fungi and mammals, adapted from (64). Early steps in the pathway until the formation of dihydroceramide are common between fungi and mammals. On the blue background are represented synthesis of inositol-containing sphingolipids, whereas on the brown background are represented synthesis of glucosylceramides. On the other hand, on green background are represented the production of glycosphingolipids by mammals……..... **9**

Figure 1.5. Glucosylceramide pathway of *Aspergillus nidulans*, adapted from (77). On the light grey background are represented sphingoid bases that can be released from ceramide moiety by action of ceramidases…… **10**

Figure 3.1. Schematic illustration of the amplified PCR products sizes of wild-type and ΔAN4405 and ΔAN4592 candidate colonies, and their respective digestion products with HpaI and ApaI enzymes (restriction sites are shown by red arrows, respectively A and B). The resulting undigested and digested PCR products were run on an agarose gel and the differential fragments sizes lead to the identification of colonies with gene disruption (a and b). The sizes of the obtained bands were compared to NZYDNA Ladder III…… **28**

Figure 3.2. Schematic illustration of the band sizes of the amplified PCR products from ΔAN5688, AN7375 and ΔAN8806 candidate colonies and wild-type, and their respective digestion with BglII (A and B) and NcoI (C) enzymes, whose restriction sites are shown by red arrows. The resulting undigested and digested PCR products were run on an agarose gel and the differential fragments sizes lead to identification of colonies with gene disruption (a, b and c). The sizes of obtained bands were compared to NZYDNA Ladder III (a and c) NZYDNA Ladder VIII and (b)…….. **29**

Figure 3.3. Chromatographic profile (HPLC) of sphingoid bases from the lipid extract of mycelia of *A. nidulans* wild-type strain (A) and mutant strains and mutant strains ΔAN4405 (B), ΔAN4592 (C), ΔAN5688 (D), ΔAN7375 (E) and ΔAN8806 (F) after 24 hours of growth in minimal medium without stress imposition. PHS = phytosphingosine; SPH = sphingosine; DHS = dihydrosphingosine; α = unknown compound with retention time at 3.8 min; x = unknown compound with retention time at 9.55 min; y = unknown compound with retention time at 11.55 min. **The scale of energy is different in each chromatogram**…… **31**

Figure 3.4. Susceptibility of GlcCer biosynthetic pathway mutants to [C_{10}mim]Cl in solid medium. The indicated amount of conidia was point inoculated in minimal medium supplemented or not (control) with 0.075 or 0.1 mM of [C_{10}mim]Cl and grown for 48h at 30 ºC (A). The growth inhibition caused by the ionic liquid was determined through growth diameter measurements. The results are the average of three repetitions ± SD. The variance was analysed by one-way ANOVA and the significant differences in inhibition of each mutant compared to the wild-type for the same condition represented, *****P ≤ 0.05, ******P ≤ 0.01, *******P ≤ 0.001 and $^{\#}$P ≤ 0.0001, (B)…….. **33**

Figure 3.5. Susceptibility of GlcCer biosynthetic pathway mutants to [$P_{4\,4\,4\,12}$]Cl in solid medium. The indicated amount of conidia was point inoculated in minimal medium supplemented or not (control) with 0.015 or 0.020 mM of [$P_{4\,4\,4\,12}$]Cl and grown for 48h at 30 ºC (A). The growth inhibition caused by the ionic liquid was determined through growth diameter measurements. The results are the average of three repetitions ± SD. The variance was analysed by one-way ANOVA and the significant differences in inhibition of each mutant compared to the wild-type for the same condition represented, *****P ≤ 0.05, ******P ≤ 0.01, *******P ≤ 0.001 and $^{\#}$P ≤ 0.0001, (B)……. **34**

Figure 3.6. Susceptibility of GlcCer biosynthetic pathway mutants to cholinium decanoate in solid medium. The indicated amount of conidia was point inoculated in minimal medium supplemented or not (control) with 1.0 or 1.25 mM of cholinium decanoate and grown for 48h at 30 ºC, the withe circles mark the colonies where slight growth was observed (A). The growth inhibition caused by the ionic liquid was determined through growth diameter measurements. The results are the average of three repetitions ± SD. The variance was analysed by one-way ANOVA and the significant differences in inhibition of each mutant compared to the wild-type for the same condition represented, *****P ≤ 0.05, ******P ≤ 0.01, *******P ≤ 0.001 and $^{\#}$P ≤ 0.0001, (B)…….. **35**

Figure 3.7. Chromatographic profile (HPLC) of sphingoid bases from the lipid extract of mycelia after 4 hours of incubation of A. nidulans wild-type strain and mutant strains in control media, without stress imposition: ΔAN4405 and ΔAN4592 (A); ΔAN5688, ΔAN7375 and ΔAN8806 (B). PHS = phytosphingosine; SPH = sphingosine; DHS = dihydrosphingosine; α = unknown compound with retention time at 3.8 min; x = unknown compound with retention time at 9.55 min; y = unknown compound with retention time at 11.55 min; z = unknown compound with retention time at 11.15 min. **The scale of energy is different in each chromatogram**…….. **36**

Figure 3.8. Chromatographic profile (HPLC) of sphingoid bases from the lipid extract of mycelia after 4 hours of incubation of A. nidulans wild-type strain and mutant strains in media supplemented with [C10mim]Cl (A and B) or [P4 4 4 12]Cl (C and D): ΔAN4405 and ΔAN4592 (A and C); ΔAN5688, ΔAN7375 and ΔAN8806 (B and D). PHS = phytosphingosine; SPH = sphingosine; DHS = dihydrosphingosine; α = unknown compound with retention time at 3.8 min; β = unknown compound with retention time at 4.1 min; i = unknown compound with retention time at 8.0 min; ii = unknown compound with retention time at 8.4 min; x = unknown compound with retention time at 9.55 min. **The scale of energy is different in each chromatogram**……. **37**

Figure 3.9. Chromatographic profile (HPLC) of sphingoid bases from the lipid extract of mycelia after 4 hours of incubation of A. nidulans wild-type strain and mutant strains in media supplemented with cholinium decanoate: ΔAN4405 and ΔAN4592 (A); ΔAN5688, ΔAN7375 and ΔAN8806 (B). PHS = phytosphingosine; SPH = sphingosine; DHS = dihydrosphingosine; α = unknown compound with retention time at 3.8 min; x = unknown compound with retention time at 9.55 min. **The scale of energy is different in each chromatogram**…….. **38**

Figure 3.10. Susceptibility of Aspergillus nidulans mutants to antifungal drugs. The best-fit EC50 values ± SD for itraconazole (A), fluconazole (B), amphotericin B (C), terbinafine (D) and flucytosine (E) were obtained by nonlinear regression analysis. The variance was analysed by one-way ANOVA and the significant differences for each mutant when compared to the wild-type represented, *P ≤ 0.05, **P ≤ 0.01 ***P ≤ 0.001 and #P ≤ 0.0001……..... **39**

Table Index

Table 2.1. Genotype description of *Aspergillus nidulans* strains used in this study. [a] Fungal Genetics Stock Center, Kansas City, MO, USA…….. **15**

Table 2.2. List of primers used for the generation of *Aspergillus nidulans* gene-replacement mutants for AN4405, AN4592, AN5688, AN7375 and AN8806……... **18**

Table 2.3. Summary of annealing temperatures used in flanking, fusion and diagnostic PCRs…….. **19**

T**able 3.1** Values of obtained minimal inhibitory concentrations of the three tested ionic liquids against *Aspergillus nidulans* mutants and wild-type strains, after growth in liquid minimal medium for 6 days... **32**

Table 4.1. Summary of data present in Figure 3.3 that demonstrated the chromatographic profile of lipid extracts from cultures after 24 hours of growth without stress imposition. ↑ Indicates level of accumulation and ─ indicates that no noticeable accumulation of compound was observed. PHS = phytosphingosine; SPH = sphingosine; DHS = dihydrosphingosine. *PHS peak may correspond to two sphingoid bases, PHS and 4,8-sphingadienine…….. **44**

Table 4.2. Summary of data present in Figure 3.8 (A and C) that demonstrated the chromatographic profile of lipid extracts from cultures after 4 hours of stress imposition by [C_{10}mim]Cl. ↑ and ↓ indicates increase and decrease, respectively, of accumulation compared to control (without stress imposition, Figure 3.7), **=** indicates similar level of compound compared to control and ─ indicates that no noticeable accumulation was observed. PHS = phytosphingosine; SPH = sphingosine; DHS = dihydrosphingosine. *****PHS peak may correspond to two sphingoid bases, PHS and 4,8-sphingadienine. [#]Compound ***x*** may correspond to the sphingoid base 9-methyl-4,8-sphingadienine…… **45**

Table 4.3. Summary of data present in Figure 3.8 (C and D) that demonstrated the chromatographic profile of lipid extracts from cultures after 4 hours of stress imposition by [$P_{4\,4\,4\,12}$]Cl. ↑ and ↓ indicates increase and decrease, respectively, of accumulation compared to control (without stress imposition, Figure 3.7), **=** indicates similar level of compound compared to control and ─ indicates that no noticeable accumulation was observed. PHS = hytosphingosine; SPH = sphingosine; DHS = dihydrosphingosine. *****PHS peak may correspond to two sphingoid bases, PHS and 4,8-sphingadienine. [#]Compound ***x*** may correspond to the sphingoid base 9-methyl-4,8-sphingadienine…… **46**

Table 4.4. Summary of data present in Figure 3.9 (A and B) that demonstrated the chromatographic profile of lipid extracts from cultures after 4 hours of stress imposition by cholinium decanoate. ↑ and ↓ indicates increase and decrease, respectively, of accumulation compared to control (without stress imposition, Figure 3.7), **=** indicates similar level of compound compared to control and ─ indicates that no noticeable accumulation was observed. PHS = phytosphingosine; SPH = sphingosine; DHS = dihydrosphingosine. *****PHS peak may correspond to two sphingoid bases, PHS and 4,8-sphingadienine. [#]Compound ***x*** may correspond to the sphingoid base 9-methyl-4,8-sphingadienine…… **48**

Table 4.5. Summary of data present in Figure 3.9 that demonstrated the EC_{50} (drug concentration producing 50 % of the effect). ↑ and ↓ indicates increase and decrease, respectively, of the EC_{50} values compared to wild-type strain, **=** indicates similar EC_{50} values compared to wild-type…… **49**

List of Acronyms

$[C_{10}mim]Cl$	1-decyl-3-methylimidazolium chloride
$[P_{4\,4\,4\,12}]Cl$	Dodecyltributylphosphonium chloride
AIDS	Acquired Immune Deficiency Syndrome
ANOVA	Analyses of variance
BLAST	Basic Local Alignment Search Tool
DG18	Dichloran-Glycerol
DHS	Dihydrosphingosine
DMSO	Dimethyl sulfoxide
dNTP	Deoxynucleotide triphosphate
EC_{50}	Half Maximal Effective Concentration
EDTA	Ethylenediaminetetraacetic acid
FGSC	Fungal Genetics Stock Center
GlcCer	Glucosylceramide
GS-MS	Gas Chromatography-Mass Spectrometry
HIV	Human Immunodeficiency Virus
HPLC	High Performance Liquid Chromatography
IL	Ionic liquid
IPC	Inositol phosphorylceramide
MIC	Minimal Inhibitory Concentration
MOPS	Morpholinepropanesulfonic acid
MTT	3-(4,5-dimethylthiazol-2-yl)-2,5-diphenyltetrazolium bromide
NCCLS	National Committee for Clinical Laboratory Standards
NMR	Nuclear Magnetic Resonance
PABA	*p*-aminobenzoic acid

PCR	Polymerase Chain Reaction
PEG	Polyethylene glycol
PHS	Phytosphingosine
ROS	Reactive Oxygen Species
SD	Standard Deviation
SPH	Sphingosine
UPLC	Ultra Performance Liquid Chromatography

CHAPTER 1 – Introduction

1.1 The Fungal Kingdom 2

1.2 Fungal Taxonomy 3

1.3 *Aspergillus nidulans* 5

1.4 Antifungal Drugs 6

1.5 Sphingolipid Biosynthesis 8

1.6 Ionic Liquids 10

1.7 Objectives 12

1.1 The Fungal Kingdom

Fungi are an ancient and unique group of eukaryotic organisms that includes yeasts, moulds and the more familiar mushrooms. These organisms are different from all others in their behaviour and cellular organisation; their uniqueness is reflected in the fact that they represent one of the three evolutionary branches of multicellular organisms (1). While some features are unique to fungi (*e.g.* rigid cell wall composed of chitin and glucans and plasma membranes containing ergosterol), they also share some morphological and biochemical characteristics with other eukaryotes (2).

Fungal cells, like in other eukaryotic organisms, present a membrane-bound nucleus containing DNA with non-coding regions (introns), sterol-containing membranes, 80S ribosomes, intracellular organelles such as mitochondria, and endomembrane systems that include the endoplasmic reticulum, Golgi apparatus, elongated vacuoles and small spherical vesicles (1,3). Nutritionally, fungi are heterotrophic organisms that require carbon as an energy source. The nutrients are acquired by extracellular digestion of complex compounds through enzymes that are secreted into the environment and then the simpler and soluble molecules are able to cross cell boundaries, being absorbed (4).

Due to their diverse cellular morphology, fungi have the ability to adapt and grow in a wide range of environments (5). During vegetative growth, fungi most commonly grow as a system of highly branching polarised tubes, forming hyphae or pseudohyphae, which together make up a network called mycelium. Some can grow as discrete yeast cells, spherical, ellipsoidal or cylindrical, which reproduce by forming buds on its surface. Few species, particularly animal and plant pathogens, can assume both morphologies switching between hyphal and yeast growth forms; this phenomenon is known as dimorphism (4,6). Changes in environmental conditions, such as exhaustion of nutrients or the death of the host, can trigger sexual or asexual development, both leading to the production of spores that have the role of propagation and/or survival (7). Asexual sporulation of fungi occurs when a nucleus divides by mitosis, producing a high number of genetically identical spores (8). Sexual sporulation is widespread in fungi, but not all groups have a known sexual stage. These extremely resistant spores are produced by meiosis, which guarantees higher genetic variability when compared to the parental cells (3,9).

Fungi can be found in all types of environments, where they play an important role in the ecosystem. For example, as saprophytes they perform the essential role of nutrient cycling, decomposing dead organic matter (10). Fungi can possess several close biological associations with other organisms, called symbiosis, in which both contributors can benefit from the relationship – mutualism (*e.g.* lichens and mycorrhizas) (3,11) or where only the fungi benefits at the expense of the other living organism – parasitism (able to become or not a pathogen, *i.e.* disease-causing agent) (1).

Besides their role in the ecosystem, fungi have a high economic impact on agriculture, medicine and industry. For centuries the yeast *Saccharomyces cerevisiae* has been widely utilised to make bread, ferment wine and brew beer (3). Mushrooms are consumed in many countries, the most produced species

being *Agaricus bisporus* (known as white or button mushroom), *Lentinula edodes* (commonly called shiitake), *Pleurotus ostreatus* (oyster mushroom) and *Flammulina velutipes* (golden needle mushroom) (12). In addition, fungal organisms have been used in the production of valuable commodities such as antibiotics (*e.g.* penicilins), vitamins (*e.g.* riboflavin (B_2), ergosterol (provitamin D_2), pharmaceutical compounds (*e.g.* cyclosporin A), fungicides, enzymes, among others (13). Although some fungi are important enhancers of crop development, as they are able to increase biotic and abiotic stress tolerance and improve plant growth (*e.g. Piriformospora indica* is capable of mimicking arbuscular mycorrhizal fungi and induces disease resistance and stress tolerance) (14,15), several pathogenic species are responsible for destroying entire crops and leading to huge economic losses (16).

Fungi are also utilised as model organisms in biology, biochemistry and especially in genetic studies, due to their intrinsic characteristics. The simple nutrient requirement, high growth rates, very large numbers of progeny, short life cycles and small genome size are some of their most favourable features (17). Furthermore, because they are eukaryotes and display many properties and functions similar to human cells, they constitute a better model for many cellular processes than bacteria. Among the examples of fungal model organisms we can find *Neurospora crassa*, *Aspergillus nidulans*, *Coprinus cinereus* and *S. cerevisiae* (18).

1.2 Fungal Taxonomy

Since ancient times that all life was divided into plants and animals, but with the evolution of the classification systems new Kingdoms were introduced. Although for long time fungi have been classified together with plants, they are more closely related to animals (19). Nowadays, fungi are classified in their own separate kingdom, Kingdom *Fungi* (20). In the six kingdom system proposed by Cavalier-Smith in 1998, only “true fungi” were included in this Kingdom, oomycetes and slime moulds being placed in the Kingdoms Chromista and Protozoa, respectively (21,22). Fungal classification and phylogeny is currently in a state of flux. At its simplest level, the classification proposed by Hibbett *et al.* accepts one subkingdom, seven phyla and ten subphyla (23), represented in Figure 1.1. The proposed phyla are: *Microsporidia*, *Chytridiomycota*, *Blastocladiomycota*, *Neocallimastigomycota* and *Glomeromycota*. The subkingdom *Dikarya* comprises the majority of described fungal species and the taxon is composed of the phyla *Ascomycota* and *Basidiomycota* (24).

Ascomycota, with approximately 64 000 known species, is the major phylum of Fungi and one of the most varied and ubiquitous phyla of eukaryotes (25). What characterises the *Ascomycota* is that their sexual spores (ascospores) are formed within a sac-like structure hyphal cell, called ascus (26). In the classification proposed by Hibbett *et al*., the phylum is subdivided into three main subphyla: *Taphrinomycotina, Saccharomycotina* and *Pezizomycotina* (23).

The most basal group *Taphrinomycotina* comprises a varied collection of organisms, including the filamentous plant pathogen *Taphrina* and the fission yeast *Schizosaccharomyces pombe* that over the years has been widely used as a model organism in cell and molecular biology. The human pathogen *Pneumocystis* and the widely distributed genus *Neolecta* are also placed in this subphylum (26,27). The *Saccharomycotina* contains a single order which includes the majority of the ascomycetous yeasts, comprising the economically important genus *Saccharomyces* and the pathogenic *Candida* species (28). The filamentous *Ascomycota* are contained in the subphylum *Pezizomycotina* that comprises a wide diversity of fungal species and life-styles (29). Included in this group are the *Aspergillus* and *Penicillium* genera, whose asexual phases are crucial in biotechnological applications. Some *Aspergillus* species, especially *A. fumigatus*, are also significant pathogens of immune-compromised human patients (27).

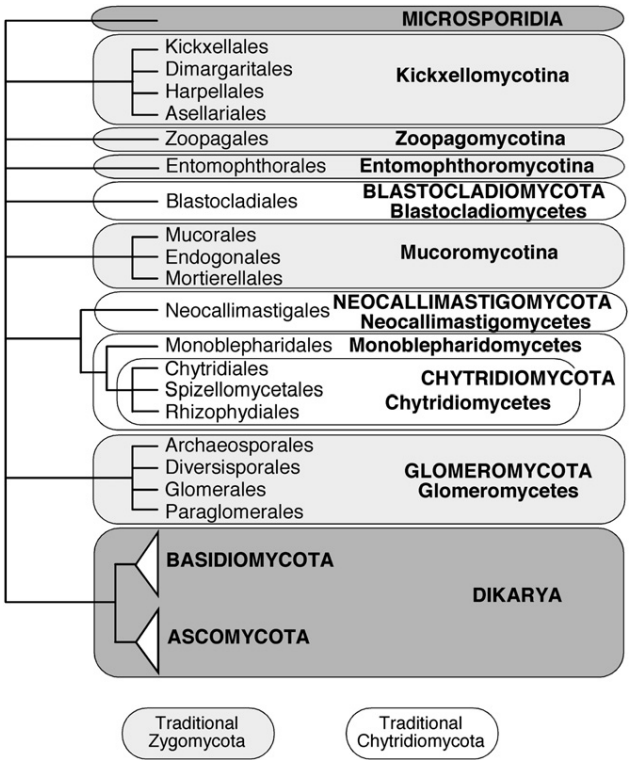

Figure 1.1. Phylogeny and classification of the Kingdom Fungi, according to Hibbett *et al*. (23). Branch lengths are not proportional to genetic distances.

The greatest diversity of fungi has emerged through processes of evolutionary change over hundreds of billions of generations and the exact number of species is incredibly difficult to predict. One commonly cited estimate, by Hawksworth in 1990, suggests at least 1.5 million different species of fungi (30), but a more recent valuation proposes a greater number, between 2.2 and 3.8 million fungal species. Despite the high number of predicted fungal species, only about 120,000 have been described to date (31), thus it is still necessary to understand the real complexity and potential of this microorganisms.

1.3 *Aspergillus nidulans*

Aspergillus is a common and widespread genus including about 250 species, 50 of which were only described after the year 2000 (32). The name of the genus derived from its similarity in appearance between the microscopic anatomy of the spore-bearing structure and an instrument used for sprinkling holy water in the Roman Catholic Church, called aspergillum (33). *Aspergillus* fungi are predominantly used in food industry (*e.g. A. oryzae* is used for the fermentation of soybeans, rice, grains and potatoes) and large-scale production of enzymes, organic acids (*e.g.* 99% of citric acid is produced worldwide by *A. niger*) and bioactive compounds (34). While most of *Aspergillus* species do not represent a threat to humans, some are known opportunistic pathogens, amongst which the most important pathogenic strains are *A. fumigatus*, followed by *A. flavus*, *A. niger*, and *A. terreus* (32). Throughout this thesis the focus of discussion will be the filamentous fungus *A. nidulans*.

Since the 1930s, *A. nidulans* has been extensively studied and, since the 70s, excellent molecular genetic tools have been developed (gene deletions, promoter replacements and production of fluorescent protein fusions), and the complete sequence and annotation of this fungus genome was accomplished in 2005 (33,35). Also, its biological features (*e.g.* haploid genome, simple nutritional requirements, rapid growth and reproduction, among others) have made *A. nidulans* an excellent model organism for studying a number of important processes such as mitosis, gene regulation, cell cycle, differentiation of conidia (asexual spores) and secondary metabolism (36,37).

A schematic representation of the *A. nidulans* life cycle is shown in Figure 1.2. *A. nidulans*, like most filamentous fungi of the Ascomycota, has an asexual cycle, in which a spore with a single nucleus germinates into a multinucleated hypha that divides and branches, forming a vegetative mycelium. On appropriate conditions, specialised hyphae called conidiophores are formed. Within the conidiophore the nucleus divides mitotically producing many haploid unicellular spores, the conidia. Upon release, conidia germinate into vegetative growing hyphae and the cycle continues (18,38). *Aspergillus nidulans* can also reproduce sexually, which begins when growing hyphae fuse and differentiate into a developing fruiting body - called cleistothecia - containing the asci. These asci bear the ascospores or sexual spores that after being released will remain on a state of dormancy, germinating only when the environmental or nutritional conditions are appropriate (18,39). In addition to these cycles, a parasexual cycle offers the genetic benefits of meiosis through a mitotic route. This cycle is initiated when haploid nuclei fuse in the vegetative cells and continue to divide mitotically (38).

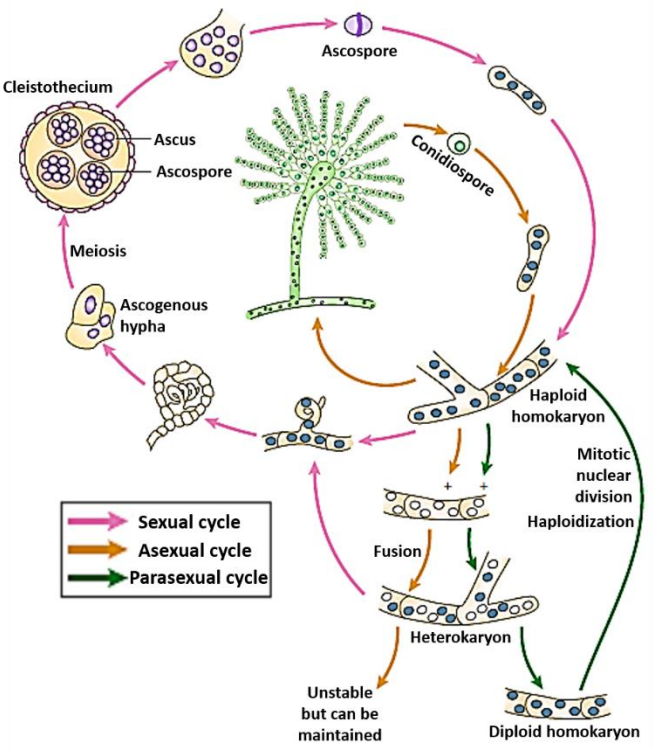

Figure 1.2. Schematic representation of *Aspergillus nidulans* life cycle adapted from (38). The sexual, asexual and parasexual cell cycles are indicated by the purple, orange and green arrows, respectively.

1.4 Antifungal Drugs

During the last few decades, filamentous fungi have been considered an increasing concern due to the rise of life-threating fungal infections. These can be divided in two categories: superficial mycoses that mostly affect skin, nails and mucosa; and invasive fungal infections like aspergillosis that affect mostly the lungs, but also other organs (40). Despite the availability of several antifungal drugs, invasive fungal infections are associated with high mortality rates, killing about one and a half million people every year (41). The increasing number of diseases caused by fungi is mostly related to the growth of the population at risk. This includes mainly immunocompromised individuals, such as HIV/AIDS, cancer, transplant and diabetes patients (42,43). Despite the increasing need for efficient antifungal treatment, mainly four classes of drugs are clinically used to treat invasive fungal infections: polyenes, azoles, echinocandins and pyrimidine analogues (44).

Polyenes are the oldest class of antifungal drugs, but only three, nystatin, natamycin and amphotericin B, are currently utilised in a clinical background. Their primary mechanism of action is the disruption of the fungal cell membrane structure through binding to ergosterol, a specific sterol of fungi (45). While amphotericin B is used for the treatment of systemic infections, nystatin and natamycin are only used as topical agents (46). Polyenes are fungicidal and compared to other antifungals have the broadest spectrum of activity; however, they also possess a slight affinity for cholesterol (sterol present in human

cells), which results in high toxicity and in numerous side effects to patient cells (45). In the last years, efforts have been made to develop new formulations with improved solubility and lower toxicity to humans (47,48).

Azoles are the most common antifungal drugs in clinical use. They indirectly affect the fungal cell membrane through inhibition of ergosterol biosynthesis (45). The first developed azoles were imidazoles; however due to their high toxicity, side effects and many interactions with other drugs, they were replaced by triazoles (49). The first generation of triazoles, itraconazole and fluconazole, displayed a broader spectrum of antifungal activity and improved safety profile, but resistance cases have increasingly been reported, which led to the development of the second generation of triazoles, such as voriconazole, posaconazole and ravuconazole (50,51).

The most recently discovered antifungal class was the echinocandins. They have a unique mechanism of action, which consists in inhibiting the synthesis of β-1,3-D-glucan, a key component of the cell wall of fungi. The echinocandins currently in clinical use are anidulafungin, caspofungin and micafungin, all of which possess a potent broad fungicidal activity and are specifically used against *Candida* and *Aspergillus* species (52).

In addition to the antifungal drugs mentioned above there are others in clinical use. As example, one of the oldest antifungal agents is 5-fluorocytosine (flucytosine), a pyrimidine analogue which mechanism of action relies on interface with DNA and RNA synthesis. Flucytosine is principally used in combination with a number of azole antifungal agents (53).

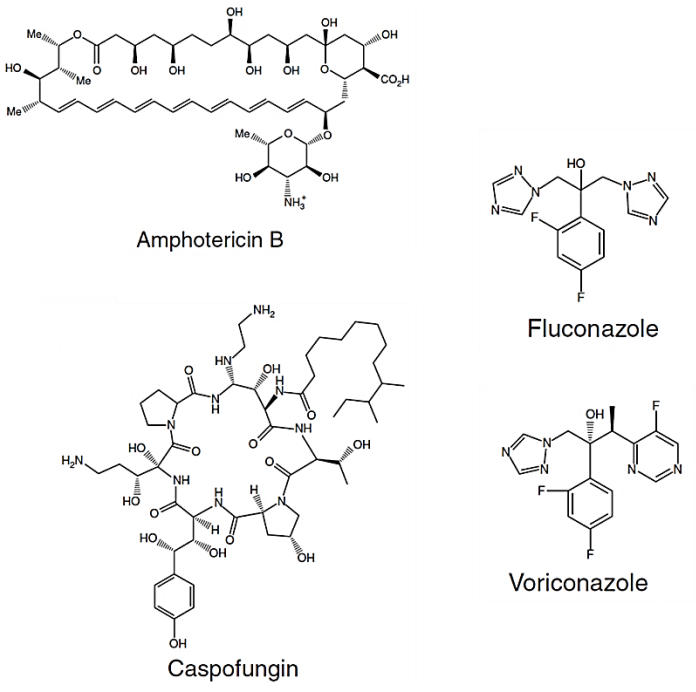

Figure 1.3. Structure of representative examples of antifungal drugs in current clinical use, adapted from (44).

The emergence of resistance to the currently used antifungal drugs and, in the most concerning cases, multidrug resistance, is reported more and more frequently, challenging the efficacy of the treatments in a near future (54-56). The currently available antifungal drugs do not meet the increasing requirements for dealing with a rising number of life-threating fungal infections; hence, the discovery of new specific antifungal targets is urgently needed. In this context, fungal sphingolipids have emerged as potential targets for the development of new antifungal agents (57).

1.5 Sphingolipid Biosynthesis

Sphingolipids are essential components of all eukaryotic cell membranes, but they are structurally distinct in mammalian and fungal cells. These molecules play an important role in a variety of biological processes like heat stress response, signal transduction and apoptosis (58-60). Furthermore, sphingolipids such as inositol phosphorylceramide (IPC) and glucosylceramide (GlcCer) play a key role in fungal pathogenesis: recent studies have shown that inhibition of the synthesis of these sphingolipids can attenuate the virulence of *Candida* and *Aspergillus* species (61,62).

The structure of sphingolipids generally comprises a sphingoid base backbone linked to a long-chain fatty acid (63). They can also further incorporate glucose, mannose and/or inositol-phosphate residues, classifying them as complex sphingolipids. There is a large diversity of sphingolipids, but while in mammalian cells the most frequent are sphingomyelins, in fungal cells there are mainly two described groups: IPCs and GlcCer (64,65).

The sphingolipid biosynthetic pathway has been characterised in great detail for the yeast *S. cerevisiae* (Figure 1.4) (66), however, knowledge of this pathway in filamentous fungi, such as *A. nidulans,* is still rather limited. The first step of sphingolipids biosynthesis is conserved among mammals and fungi, starting by the condensation of a serine and palmitoyl-CoA or stearyl-Coa, forming 3-ketodihydrosphingosine (67). The sphingoid bases dihydrosphingosine and phytosphingosine are the following products (68). They can then be condensed with a very-long chain fatty acid to yield dihydroceramide and phytoceramide, a reaction catalysed by ceramide synthases (63,69). From these two structures, IPCs and GlcCer are then formed. IPC, the first complex sphingolipid, is formed by the addition of an inositol phosphate group to phytoceramide. Next, IPC can be converted to mannose-inositolphosphoryl ceramide, and addition of a second inositol phosphate group to the former yields mannosediinositolphosphoryl ceramide – the most complex product of this pathway (63,70,71). Detailed GlcCer pathway of *A. nidulans* is shown in Figure 1.5. It initiates with a Δ4-desaturation of the sphingoid backbone of dihydroceramide, followed by Δ8-desaturation of the subsequent sphingoid backbone. Next, a sphingolipid C9-methyltransferase catalyses the introduction of a methyl group at the C9 position (72,73). The last step to synthesise glucosylceramide consists of the transfer of a glucose residue from UDP-glucose to the ceramide moiety by a glucosylceramide synthase (74).

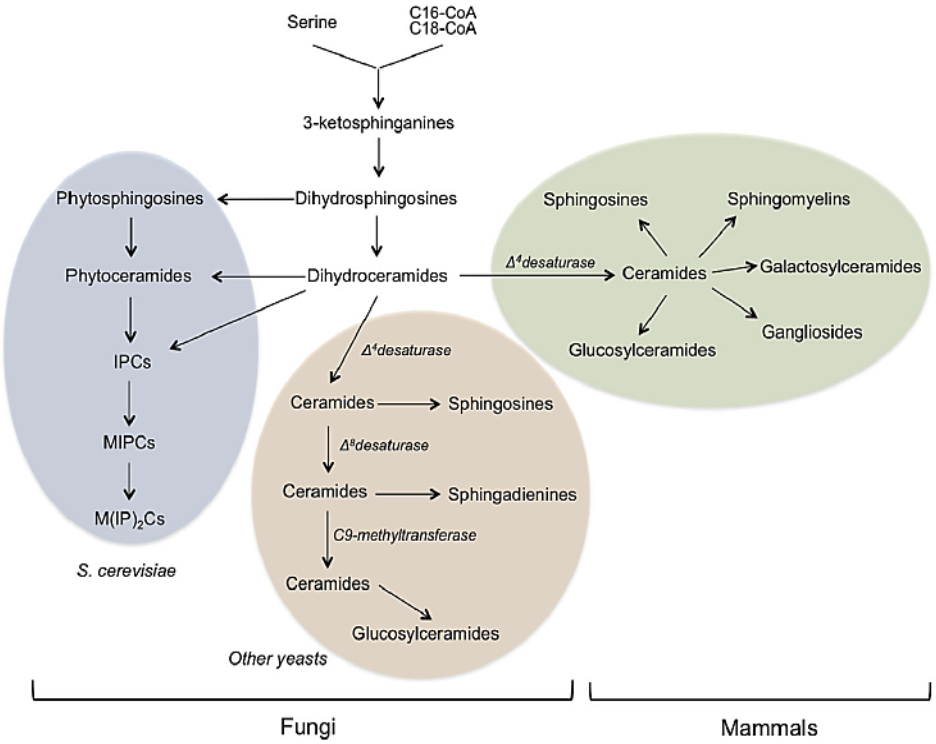

Figure 1.4. Overview of the sphingolipid biosynthetic pathways in fungi and mammals, adapted from (65). Early steps in the pathway until the formation of dihydroceramide are common between fungi and mammals. On the blue background are represented synthesis of inositol-containing sphingolipids, whereas on the brown background are represented synthesis of glucosylceramides. On the other hand, on green background are represented the production of glycosphingolipids by mammals.

Studies have shown that the intermediates of GlcCer synthesis can play important roles in fungal cells. In *Candida albicans* the disruption of Δ8-desaturase leads to reduction of hyphal growth, which is a consequence of the accumulation of 4-sphingenine, also known as sphingosine (75). Moreover, mutation of the sphingolipid C9-methyltransferase gene in *Cryptococcus neoformans* alters membrane composition and affect the fungal membrane rigidity (76). Two genes encoding sphingolipid C9-methyltransferases, Fg*MT1* and Fg*MT2* were identified in the fungal pathogen *Fusarium graminearum*, and strains lacking the Fg*MT2* gene exhibit severe growth defects and produce abnormal conidia (77). In the filamentous fungus *A. nidulans,* genes coding for sphingolipid Δ8-desaturase, two sphingolipid C9-methyltransferases and glucosylceramide synthase were identified. Data showed that deletion of these genes promoted resistance to cell-wall-damaging agents. However, deletion of sphingolipid Δ8-desaturase gene led to a significant reduction of growth (78).

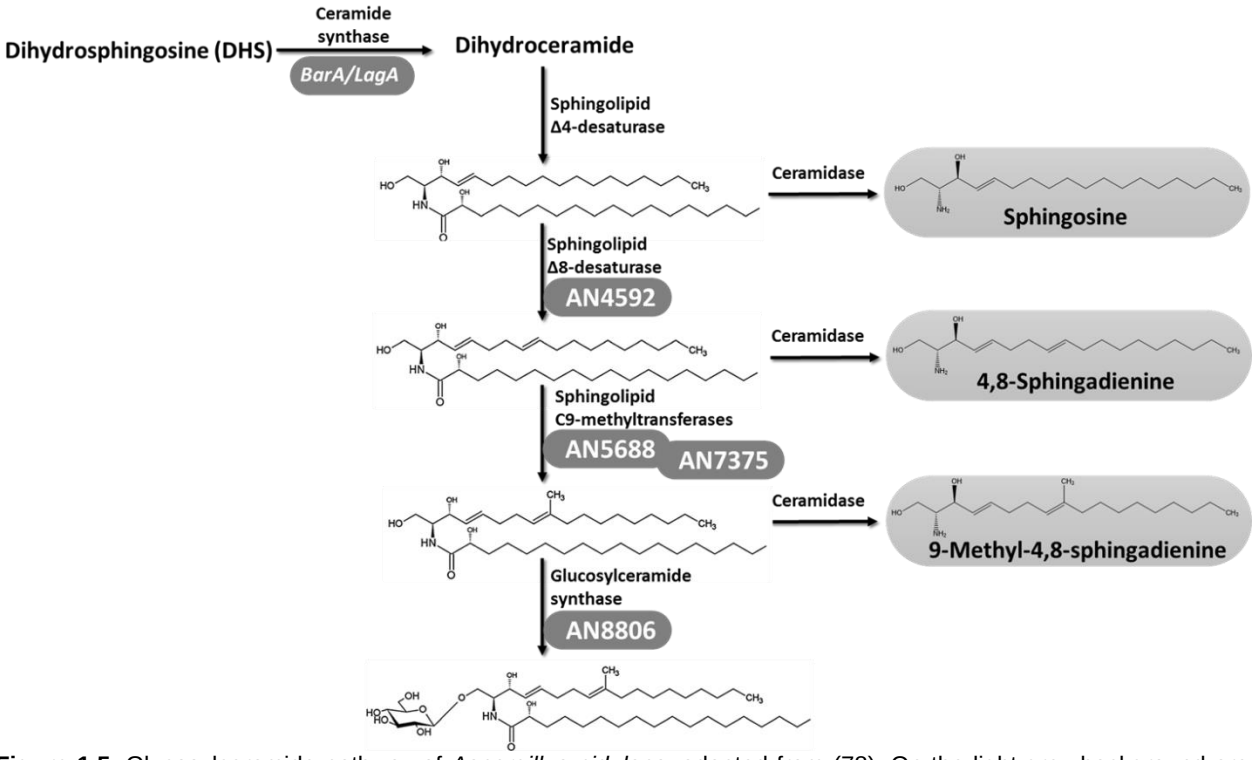

Figure 1.5. Glucosylceramide pathway of *Aspergillus nidulans*, adapted from (78). On the light grey background are represented sphingoid bases that can be released from ceramide moiety by action of ceramidases.

Previous work developed by our team showed that some ionic liquids that cause membrane permeabilisation and cell wall damage also activate the sphingolipid biosynthetic pathway, leading to accumulation of certain intermediates. Curiously, each family of ionic liquids tested seem to induce distinct profiles of sphingoid bases accumulation, including unknown species (analysed by liquid chromatography) (79). The hypothesis is that these unknown accumulated sphingoid bases may be the intermediates of the synthesis of GlcCer. Additionally, these sphingoid bases could be involved in the activation of the cell wall integrity pathway in *A. nidulans*.

1.6 Ionic Liquids

Ionic liquids (ILs) are a class of compounds that have become a hot topic since the mid-1990s. Due to their unique physicochemical characteristics, these compounds have shown increasingly promising perspectives in the diverse fields of synthesis, catalysis/biocatalysis, material science, among others (80). By definition, ILs are a class of organic salts completely constituted by ions that have a melting point below 100 ºC (81). Usually, they consist of a large asymmetrical organic cation associated with a polyatomic anion that may be organic or inorganic. Millions of formulations of ILs are possible through structural modifications in the cation or the anion, which allows alterations of their physical and chemical properties. Thus, the tunability of ILs is

a great advantage relatively to conventional molecular organic solvents (82,83). Other properties that make ILs very attractive and to be considered as “green solvents” are their high thermal stability, good solvation properties and extremely low vapour pressure (84). However, not all ILs are “green” or environmentally friendly. To define which ILs can be consider “green”, many studies have been performed in order to assess their environmental impact and biodegradability (81).

Imidazolium-based ionic liquids were one of the first to find application on an industrial scale and probably are the most investigated group (81). Early eco-toxicological analyses performed on imidazolium-based ionic liquids focused on their antimicrobial properties against relevant microbial strains, where an increasing toxicity trend with the elongation of an alkyl chain was observed (85). These initial studies stimulated toxicity-based investigations in other biological models. For example, the toxic effect of imidazolium-based ILs was tested on the crustacean *Daphnia magna* survival (86), two green algae *Chlorella vulgaris* and *Oocystis submarina*, and the marine diatoms *Cyclotella meneghiniana* and *Skeletonema marinoi* (87). Furthermore, their toxic effects were also analysed against leukaemia and glioma rat cell lines (88) and human HeLa cell lines (89). A correlation was proposed between the toxicity and the 1-octanol/water partition coefficient of the cation, suggestive of increasing lipophilicity, with elongation of the alkyl side chain leads to greater interaction with biological membranes (90).

Another group of ILs of great interest is the quaternary ammonium salts, including ILs-based in the benign cholinium cation (91). It was proved that the cholinium-based ionic liquids can be biocompatible, including cholinium alkanoates, which have shown low toxicity against filamentous fungi from the genus *Penicillium* (92) and human cell lines (93), and also high biodegradability (92).

Cationic groups such as the quaternary phosphonium are attracting interest in ionic liquid research. Despite their high industrial interest, the information about their hazards to the environment is still limited and not conclusive (94). Also, this group of ILs showed low levels of biodegradability (95) and in the marine bacteria *Vibrio fischeri* they appear to be more toxic than the analogue imidazolium-based ILs (94). Studies of toxicity of alkyltributylphosphonium chlorides towards *A. nidulans* showed that their mechanism of toxicity includes increase in plasma membrane permeabilisation and cell wall damage (96)

In our team, studies have been performed to assess the effect of some families of ionic liquids in model fungal organisms like *N. crassa* and *A. nidulans*, demonstrating the capacity of these compounds to send unique stimuli to fungi (97,98). Taken as an example, ILs seem to activate fungal specific regulatory mechanisms, that led to alterations in lipid metabolism, specifically in the synthesis of sphingolipid intermediates (79), among other effects (99).

1.7 Objectives

This thesis aimed at studying how the sphingolipid biosynthesis impacts stress responses in *Aspergillus nidulans*, a model organism that has its genome already completely sequenced and available. Previous studies showed that some ionic liquids can affect the sphingolipid biosynthetic pathway, leading to the accumulation of unknown species. It was hypothesised that the unknown accumulated sphingoid bases are intermediates of the glucosylceramide (GlcCer) biosynthetic pathway.

Primarily, this study had as objective the identification of novel genes encoding enzymes that could be involved in structural modifications of sphingoid bases from the GlcCer pathway in *A. nidulans* – a necessary step to identify compounds that influence stress response pathways in this fungus. With this in mind, we aimed at constructing strains carrying deletions in the genes coding for the GlcCer pathway and at carrying out their functional characterisation and analyses of their sphingoid base accumulation profile by liquid chromatography. Ultimately our goal was to determine, through analysis of the differential pattern of accumulation of sphingoid bases, how the deletion of GlcCer pathway genes impacts stress responses in fungi, in particular upon exposure to the ionic liquids previously observed to impact this biosynthetic pathway. We also aimed at investigating the contribution of the identified genes to *A. nidulans* susceptibility to each ionic liquid through determination of their minimal inhibitory concentrations and impact on the radial growth of the fungus.

Following the observed effects on ionic liquid stress, we also aimed at identifying how deletion on each element of the sphingolipid biosynthesis could influence the fungal response to a selected set of known antifungal drugs. The final goal was to identify intermediates of the GlcCer pathway capable of increasing the fungus susceptibility to a chemical stress; hence also to identify how the ability of ionic liquids to influence the biosynthesis of sphingolipids can be used to hamper the capacity of fungi to circumvent the stress caused by antifungal drugs. Ultimately, this would open the possibility to design ionic liquids for potentiating the fungicidal activity of conventional antifungal drugs, allowing a more efficient antifungal treatment at lower doses.

CHAPTER 2 – Materials and Methods

2.1 Chemicals 14
2.2 Strains and storage conditions 15
2.3 Culture mediums 15
2.4 Generation of deletant strains 16
2.4.1 Construction of deletion cassettes 16
2.4.2 Generation of transformable protoplasts and their transformation 19
2.4.3 Selection and confirmation 20
2.5 Determination of minimal inhibitory concentrations of ionic liquids 20
2.6 Determination of radial growth in solid medium supplemented with ionic liquids 21
2.7 Lipid content assessment 21
2.8 High performance liquid chromatography analysis 22
2.9 Determination of susceptibility to antifungal drugs 22

2.1 Chemicals

The ionic liquid 1-decyl-3-methylimidazolium chloride, [C_{10}mim]Cl, was purchased from IoLiTec Ionic Liquids Technologies and dodecyltributylphosphonium chloride, [P $_{4\,4\,4\,12}$]Cl, was custom synthesised by the same company, according to (100). The cholinium decanoate, [$NMe_3(CH_2CH_2OH)$][$C_{10}H_{21}CO_2$], was synthesised as previously described (101). Ionic liquids were characterised by ^{1}H, ^{13}C and ^{31}P NMR spectroscopy, mass spectrometry, CHN elemental analysis, and halide and water content analyses.

The compounds used in the preparation of culture mediums: uracil, uridine, pyridoxin, D(+)-glucose, thiamine hydrochloride, KCl, $MgSO_4 \cdot 7H_2O$, KH_2PO_4, $ZnSO_4 \cdot 7H_2O$, H_3BO_3, $MnCl_2 \cdot 4H_2O$, $FeSO_4 \cdot 7H_2O$, $CoCl_2 \cdot 6\ H_2O$, $CuSO_4 \cdot 5\ H_2O$, $NaNO_3$, $Na_2MoO_4 \cdot 2\ H_2O$, Na_4EDTA, biotin, riboflavin, *p*-aminobenzoic acid (PABA), nicotinic acid, RPMI-160 medium (R6504), morpholinepropanesulfonic acid (MOPS), were purchased from Sigma-Aldrich; Dichloran-Glycerol (DG18), yeast extract and peptone bacteriological were purchased from Oxoid; sucrose from Alfa Aesar; casein hydrolysate from Fluka; agar and NaCl from Panreac AppliChem; NaOH from JMGSantos and glycerol from Fisher Bioreagents. Molecular biology reagents used for PCR reactions were purchased from NZYTech. The dimethyl sulfoxide (DMSO) and 3-(4,5-dimethylthiazol-2-yl)-2,5-diphenyltetrazolium bromide (MTT) were purchased from Sigma-Aldrich and isopropanol from Labkem.

The reagents used for sphingolipid extraction: pyridine, butanol, ammonium hydroxide and 40 % methylamine in water were purchased from Acros Organics; ethanol, methanol and chloroform were purchased from Fisher Chemical and diethylether from Panreac AppliChem. Sphingoid bases standards (phytosphingosine, sphingosine and dihydrosphingosine) were purchased from Avanti Polar Lipids. All solvents used in chromatographic analyses were of the highest analytical grade and water was obtained from a Milli-Q system (Millipore).

2.2 Strains and storage conditions

The *Aspergillus nidulans* strains used in this study are described in Table 2.1. FGSC A1149, obtained from the Fungal Genetics Stock Center (Kansas City, MO, USA), served as parental strain to generate ΔAN4405, ΔAN4592, ΔAN5688, ΔAN7375, ΔAN8806 deletion mutants and was used as a wild-type control for all experiments. The strains were cultivated on Dichloran-Glycerol (DG18) agar plates supplemented with uracil (1.12 $g \cdot l^{-1}$), uridine (1.2 $g \cdot l^{-1}$) and pyridoxin (0.05 $mg \cdot l^{-1}$) for the wild-type, or only with pyridoxin (0.05 $mg \cdot l^{-1}$) for the mutant strains. Cultures were incubated in the dark, for seven days, at 30 ºC. Asexual spores (conidia) were harvested using 0.85 % (w/v) NaCl solution and filtered through miracloth. The harvested spores were resuspended in a 0.85 % (w/v) NaCl solution, to be used immediately, or in a cryoprotective solution containing 0.85 % (w/v) NaCl and 10 % (v/v) glycerol and stored at -20 ºC or -80 ºC.

Table 2.1. Genotype description of *Aspergillus nidulans* strains used in this study. [a] Fungal Genetics Stock Center, Kansas City, MO, USA

Strains	Genotype	Source	Reference
A1149 (WT)	*pyrG89; pyroA4; nkuA::argB*	FGSC[a]	(102)
ΔAN4405	*pyrG89; pyroA4; nkuA::argB;* ΔAN4405::*pyrG*^{Af}	This study	This study
ΔAN4592	*pyrG89; pyroA4; nkuA::argB;* ΔAN4592::*pyrG*^{Af}	This study	(78)
ΔAN5688	*pyrG89; pyroA4; nkuA::argB*; ΔAN5688::*pyrG*^{Af}	This study	(78)
ΔAN7375	*pyrG89; pyroA4; nkuA::argB;* ΔAN7375::*pyrG*^{Af}	This study	(78)
ΔAN8806	*pyrG89; pyroA4; nkuA::argB;* ΔAN8806::*pyrG*^{Af}	This study	(78)

2.3 Culture mediums

Due to nutritional requirements of the strains, media were supplemented with uracil (1.12 $g \cdot l^{-1}$), uridine (1.2 $g \cdot l^{-1}$) and pyridoxin (0.05 $mg \cdot l^{-1}$) for the wild-type, or only with pyridoxin (0.05 $mg \cdot l^{-1}$) for the mutant strains. **Liquid minimal medium** was prepared by dissolving, in distilled water, glucose (10.0 $g \cdot l^{-1}$), thiamine (0.01 $g \cdot l^{-1}$), 5 % (v/v) nitrate salts solution and 0.1 % (v/v) trace elements solution. The pH of the medium was adjusted to 6.5 with 1 M NaOH and then sterilised in an autoclave (115 ºC; 15 min). **Nitrate salts solution** was composed by $NaNO_3$ (120.0 $g \cdot l^{-1}$); KCl (10.4 $g \cdot l^{-1}$); $MgSO_4 \cdot 7H_2O$ (10.4 $g \cdot l^{-1}$) and KH_2PO_4 (30.4 $g \cdot l^{-1}$) in distilled water. The solution was autoclaved and stored at 4 ºC. **Trace elements solution** was prepared by dissolving in distilled water $ZnSO_4 \cdot 7H_2O$ (22.0 $g \cdot l^{-1}$); H_3BO_3 (11.0 $g \cdot l^{-1}$); $MnCl_2 \cdot 4H_2O$ (5.0 $g \cdot l^{-1}$); $FeSO_4 \cdot 7H_2O$ (5.0 $g \cdot l^{-1}$); $CoCl_2 \cdot 6\ H_2O$ (1.7 $g \cdot l^{-1}$); $CuSO_4 \cdot 5\ H_2O$ (1.6 $g \cdot l^{-1}$); $Na_2MoO_4 \cdot 2\ H_2O$ (1.5 $g \cdot l^{-1}$) and Na_4EDTA (50.0 $g \cdot l^{-1}$), the compounds were added in order and boiled until dissolved. After the solution

cooled down to approximately 60 ºC the pH was adjusted to 6.5 with KOH, and the final volume was adjusted with distilled water. The solution was stored at 4 ºC. **Selective YAS medium** was made by dissolving, in distilled water, glucose (5.0 $g \cdot l^{-1}$), yeast extract (5.0 $g \cdot l^{-1}$), sucrose (342.3 $g \cdot l^{-1}$), pyridoxin (0.05 $mg \cdot l^{-1}$), 0.1% (v/v) trace elements solution and 0.1 % (v/v) **vitamin solution**, previously prepared and containing: biotin (1.0 $g \cdot l^{-1}$), pyridoxin (1.0 $g \cdot l^{-1}$), thiamine (1.0 $g \cdot l^{-1}$), riboflavin (1.0 $g \cdot l^{-1}$), *p*-aminobenzoic acid (PABA) (1.0 $g \cdot l^{-1}$) and nicotinic acid (1.0 $g \cdot l^{-1}$), The YAS medium was jellified with 1.5 % (w/v) agar and sterilised in an autoclave (115 ºC; 15 min). **Complete medium** was made with glucose (10.0 $g \cdot l^{-1}$), peptone (2.0 $g \cdot l^{-1}$), yeast extract (1.0 $g \cdot l^{-1}$), casein hydrolysate (1.0 $g \cdot l^{-1}$), 5 % (v/v) nitrate salts solution, 0.1 % (v/v) trace elements and 0.1 % (v/v) vitamin solution, in distilled water. The medium was jellified with 1.5 % (w/v) agar and sterilised in an autoclave (115 ºC; 15 min). **Osmotic medium** was prepared by dissolving in distilled water 1.2 M $MgSO_4 \cdot 7H_2O$ and 10 Mm sodium phosphate buffer pH 6.5, the final pH of solution was adjusted with Na_2HPO_4 to 5.8. The medium was filter-sterilised and stored at 4 ºC. **RPMI 1640 medium**, was supplemented with glucose (8.0 $g \cdot l^{-1}$), 0.165 M morpholinepropanesulfonic acid (MOPS) and buffered to pH 7.0 using concentrated NaOH. For the wild-type strain the medium was additionally supplemented with uracil and uridine. The medium was filter-sterilised and stored at 4 ºC.

2.4 Generation of deletion strains

The genes AN4405, AN4592, AN5688, AN7375 or AN8806 were selected for gene replacement with *A. fumigatus pyr*G gene (*pyr*G^{Af}) in *A. nidulans* A1149 strain (Table 2.1). The construction of deletion cassettes for *A. nidulans* gene replacement was performed according to a previously established method (103). The production of transformable protoplasts, their transformation with deletion cassettes, selection of transformant colonies and confirmation of the deletion was adapted from (103-105).

2.4.1 Construction of deletion cassettes

The AN4405, AN4592, AN5688, AN7375, AN8806 deletion cassettes were constructed in our lab, using a fusion PCR (Polymerase Chain Reaction) protocol (103). To produce replacement PCR products for each gene, six oligonucleotide primers (P1-P6) were designed following the general rules of Innis and Gelfand (106). The primers were designed for each gene target based on the sequence of *A. nidulans* genes (*Aspergillus* Genome Database, http://www.aspergillusgenome.org) and analysed using the NetPrimer web tool (http://www.premierbiosoft.com/NetPrimer/AnalyzePrimer.jsp). All oligonucleotide primers used in this study are listed in Table 2.2.

PCRs reactions were performed in a T100™ Thermal Cycler (Bio-Rad). The auxotrophy marker gene *pyrG*^{Af} from *A. fumigatus* was amplified from plasmid pCDS60 (FGSC, Kansas City, MO, USA) using primers CDS164 and CDS165 (Table 2.2). One PCR reaction for each flanking fragment upstream and

downstream of the genes coding region was performed. Fragments with approximately 1 kb in length were amplified with primer pairs P1 and P3 for 5'-flank and P4 and P6 for 3'-flank, using A1149 genomic DNA as a template. Primers P3 and P4 were specifically designed such that amplifications would produce fragments that have ends complementary to the *pyr*G^{Af} fragment. The reaction mixtures were prepared in 200 µl thin-wall PCR tubes, containing 100 ng template DNA, primer pair P1 and P3 or P4 and P6 (0.3 µM each), 0.4 mM dNTPs NZYmix, 1.25 U NZYProof DNA polymerase, with a final volume of 50 µl. The PCR conditions to amplify the flanking fragments were: denaturation at 95 ºC for 2 min; 30 cycles of denaturation at 95 ºC for 20 s, ramp to 70 ºC at maximum rate, and from 70 ºC to primer annealing temperature at a rate of 0.1 ºC per s, annealing for 30 s at the temperatures described in Table 2.3, ramp to the extension temperature at 0.2 ºC per s, extension for 1 min per kb of amplified fragment at 68 ºC, final ramp at maximum rate to return to 95 ºC for template denaturation. The PCR amplification products were checked by agarose gel electrophoresis (1 % (w/v) agarose in TAE (Tris-acetate-EDTA) buffer). All PCR-amplified fragments were stored at -20 ºC until used in subsequent steps.

To produce a linear molecule for transformation, fusion PCR of the flanking regions with the *pyr*G^{Af} were performed using nested primers P2 and P5 for each gene target. The reaction mixture contained 150 ng pyrG^{Af} cassette, 150 ng 5'-flank, 150 ng 3'-flank, nested primers P2 and P5 (0.5 µM each), 0.5 mM dNTPs NZYmix, 5.0 U NZYLong DNA polymerase, at a final volume of 50 µl. The PCR conditions to amplify the linear DNA fragment for transformation were: denaturation at 95 ºC for 2 min; 10 cycles of denaturation at 95 ºC for 20 s, ramp to 70 ºC at maximum rate and from 70 ºC to primer annealing temperature at 0.1 ºC per s, annealing for 30 s at temperatures described in Table 2.3, ramp to the extension temperature at 0.2 ºC per s, extension for 1 min per kb of amplified fragment at 68 ºC, final ramp at maximum rate to return to 95 ºC for template denaturation; 5 cycles repeating previous steps except the extension time increased 5 s each subsequent cycle; and 10 cycles with extension time increasing 20 s each cycle. The final fused products were run on a 1 % agarose gel in TAE buffer, the desired band was excised from the gel with a clean scalpel and purified as described in the protocol of the NZYGelpure kit (NZYTech). Purified fusion PCR products were stored at -20 ºC until used for transformation.

Table 2.2. List of primers used for the generation of *Aspergillus nidulans* gene-replacement mutants for AN4405, AN4592, AN5688, AN7375 and AN8806.

Gene	Primer	Sequence 5' – 3'
AN4405	P1	AGGAGGCTGGAATTGATGTC
	P2	GCCGCTATCCAAGAAACTATG
	P3	ATCCACTTAACGTTACTGAAATCCGAGGATAAAGGAGGAGAAGG
	P4	GCTCCTTCAATATCATCTTCTGTCCGATTCGGATGATAACTGGG
	P5	ACCAGGGTTTGCGACAGAG
	P6	AAGCAAACCGACTACGAGACTC
AN4592	P1	ACAATCAGCAGTCTCGGTAAGC
	P2	ATTATCTTGGGCTGGGTTCTG
	P3	ATCCACTTAACGTTACTGAAATCTGGCTGTCAAGCAATAACCAG
	P4	GCTCCTTCAATATCATCTTCTGTCGTTATGCCATTGCCTTTGAC
	P5	ATTCCGATGACGACGAACG
	P6	GCCATCCTTTCTGCCCTC
AN5688	P1	TTCGACGGTCCGTGCTC
	P2	GGCAACGAGCGGACTATTC
	P3	ATCCACTTAACGTTACTGAAATCGCAACGAATTGACCAAGACG
	P4	GCTCCTTCAATATCATCTTCTGTCGTGCCTGAGTCGACAGATGAG
	P5	GGCAGTCTCTTGAATTGACGAG
	P6	CAGCAGGGTAGTAAGCGTGAC
AN7375	P1	ACCCAGGGACAACCTCGTAG
	P2	GCAGCCATGCTTCTCATACAG
	P3	ATCCACTTAACGTTACTGAAATCAGTGAAGCCTGAAGGGATGG
	P4	CTCCTTCAATATCATCTTCTGTCCTGCTGTTGGTGAATCTGTTATC
	P5	CAAGACACCTGGCGTACCTAC
	P6	TCTACCAACTGCTCGCCTTC
AN8806	P1	TCAGGCACAGTCTCTGGAGG
	P2	ATGCTTCAATCACTCATTCAGTC
	P3	ATCCACTTAACGTTACTGAAATCGTGGTCAGGTCAGGTTCAGC
	P4	CTCCTTCAATATCATCTTCTGTCGCACGGAGAAATAGAGCACG
	P5	CCTCAGATCAATCCAAATCG
	P6	CTATATCACGGCTGTGTTAGACG
pyrG^{Af}	CDS164	GATTTCAGTAACGTTAAGTGGAT
	CDS165	GACAGAAGATGATATTGAAGGAGC

Table 2.3. Summary of annealing temperatures used in flanking, fusion and diagnostic PCRs.

Gene	Annealing temperature (ºC)			
	Flanking PCR		Fusion PCR	Diagnostic PCR
	5'-Flank	3'-Flank		
AN4405	51	53	52	51
AN4592	53	51	53	52
AN5688	52	51	53	51
AN7375	53	51	52	53
AN8806	52	52	50	50

2.4.2 Generation of transformable protoplasts and their transformation

To produce transformable protoplasts, 1 x 10^8 freshly harvested conidia from A1149 strain were inoculated into 100 ml of liquid minimal medium supplemented with uracil, uridine and pyridoxin (Section 2.3). The cultures were incubated overnight (14-16 hours) at 30 ºC, 90 r.p.m. The germinated conidia were collected by centrifugation (4,500 x *g* for 5 min in a swing-bucket rotor) and then washed with a 0.6 M $MgSO_4$ solution. The washed culture was resuspended in filter-sterilised **enzymatic mix**, prepared by dissolving in 40 ml of osmotic medium (Section 2.3): 300 mg Lysing Enzymes from *Trichoderma harzianum* (Sigma-Aldrich), 150 µl β-Glucuronidase from bovine liver, type B-1 (Sigma-Aldrich) and 150 mg Driselase™ *Basidiomycetes* sp. (Sigma-Aldrich). This cell suspension was transferred to a 250 ml flask and incubated for 20 hours at 30 ºC with mild shaking (90 r.p.m). The digested germlings were recovered by centrifugation and aliquots of 10 ml of suspension were transferred to a 15 ml centrifuge tube and carefully overlayed with 5 ml of **protoplast trapping buffer** (0.6 M sorbitol and 100 mM Tris-HCl pH 7.0) and centrifuged (1,500 x *g* at 4 ºC for 15 min in a swing-bucket rotor). Protoplasts present between the two formed phases were carefully removed and washed three times with 10 ml of **ST10 buffer** (1.2 M sorbitol and 10 mM Tris-HCl pH 7.5) by centrifugation (1,000 x *g* at 4 ºC for 5 min). Protoplasts were then resuspended in 1 ml of **ST10 buffer** and kept overnight at 4 ºC. Protoplasts were centrifuged (1,000 x *g* at 4 ºC for 2 min) and the pellet resuspended in 700 µl of **STC buffer** (1.2 M sorbitol, 10 mM Tris-HCl pH 7.5 and 10 mM $CaCl_2$). For each transformation, 10 µl of cleaned fusion PCR product were added to 100 µl protoplast suspension, then vortexed 6-8 times for 1 s at maximum speed. 50 µl of freshly filtered polyethylene glycol **(PEG) solution** (25 % (w/v) in STC buffer) were added to the mixture, vortexed 4-5 times and placed in an ice bath for 25 min. Another 1 ml of filtered **PEG solution** was then added, gently mixed using a micropipette and placed at room temperature for 25 min. 100 µl of the transformation mix were plated onto primary transformation plates with selective **YAS medium.** A negative control was also performed, adding sterile water to protoplasts instead of the fusion PCR products. The selective plates were incubated for 3 or 4 days at 30 ºC.

2.4.3 Selection and confirmation

The mutant strains were selected in media without uracil and uridine, and the integration of the deletion cassette and consequent gene disruption were confirmed by PCR. Thus, from the primary transformation plates, six isolated colonies were selected and their conidia were carefully removed using a 1 µl loop previously immersed in a 0.85 % (w/v) NaCl solution. The conidia were streaked in selective **complete medium** (supplemented with pyridoxin) plates (Section 2.3) and incubated at 30 ºC for 4 days. Streaking to a single colony was repeated two more times. Conidia from a single colony were inoculated into selective complete medium plate, grown for seven days at 30 ºC then harvested and finally stored at -20 ºC as described in Section 2.2. One aliquot of conidia were taken to extract DNA for diagnostic PCR to identify which transformed colonies have the desired gene deletion. The genomic DNA was extracted as described in the extraction protocol of the used Quick-DNA™ Fungal/Bacterial Microprep Kit (Zymo Research). For each transformant and also for the control (genomic DNA of wild type), PCRs were performed, containing per reaction: 2 µl of extracted DNA, 0.5 µM of each primer P2 and P5 (Table 2.2), 0.5 mM dNTPs NZYmix (NZYTech), 5.0 U NZYLong DNA polymerase, at a final volume of 50 µl. The diagnostic PCR conditions were: denaturation at 95 ºC for 2 min; 10 cycles of denaturation at 95 ºC for 10 s, annealing for 30 s at temperatures described in Table 2.3, extension at 68 ºC for 4 min; 15 cycles repeating previous steps except the extension time increased 20 s each subsequent cycle; 1 cycles of extension at 68 ºC for 8 min. The PCR products were digested using one of the restriction enzymes ApaI, HpaI, BglII or NcoI (NZYTech). These enzymes have different restriction sites between *pyrG*^{Af} and AN4405, AN4592, AN5688, AN7375 or AN8806 genes sequences. The PCR products and the digested PCR products were run on a 1 % agarose gel in TAE buffer. This strategy led to the identification of differential DNA fragments in the wild-type and mutant strains, indicating that these genes were deleted. After the confirmation, a single null strain of each gene was selected for all the analyses.

2.5 Determination of minimal inhibitory concentrations of ionic liquids

The minimal inhibitory concentrations (MIC) of the ionic liquids [C_{10}mim]Cl, cholinium decanoate and [$P_{4\,4\,4\,12}$]Cl were determined as previously described by Hartmann *et al*. (98). The liquid **minimal medium** was prepared as described in Section 2.3. Ionic liquids were added to the minimal culture media at final concentrations ranging from 0.05 mM to 0.45 mM for [C_{10}mim]Cl, from 2 mM to 6 mM for cholinium decanoate and from 0.005 mM to 0.045 mM for [$P_{4\,4\,4\,12}$]Cl. Each liquid medium (1 ml) was inoculated with a suspension of fungal conidia, in order to obtain a final concentration of 10^6 conidia per ml, then the inoculated medium was divided into four wells (0.2 ml each) of a 96-well microtitre plate. Cultures were incubated in the dark at 30 ºC, for six days. Fungal growth or its absence was evaluated at the end of incubation, gauging by eye the formation of mycelium (turbidity). The lowest concentration that inhibited

growth was taken as the MIC. The determined values of the MIC should not be taken as absolute ones but as an indication of the upper inhibitory concentration limits.

2.6 Determination of radial growth in solid medium supplemented with ionic liquids

In dropout experiments, 1 µl of ΔAN4405, ΔAN4592, ΔAN5688, ΔAN7375, ΔAN8806 and wild-type strain suspensions containing 1×10^8, 1×10^7 and 1×10^6 conidia per ml was used to inoculate plates with **minimal medium** (described in Section 2.3, but without thiamine and jellified with 2 % (w/v) agar) supplemented with ionic liquids to obtain a range of final concentrations for $[C_{10}mim]Cl$ between 0.01 mM and 0.15 mM, for cholinium decanoate between 0.25 mM and 1.5 mM, and for $[P_{4\,4\,4\,12}]Cl$ between 0.01 mM to 0.025 mM. Fungal cultures were grown in dark for 48 h at 30 ºC, after which the size of each colony was measured and digital photographs were taken. For each condition three biological replicates were prepared. Data were compared on GraphPad 6.01 software using one-way ANOVA analysis of variance with Dunnett's test, statistical significance was considered when P values were < 0.05.

2.7 Lipid content assessment

To analyse the presence of sphingolipid intermediates that are synthesised by ΔAN4405, ΔAN4592, ΔAN5688, ΔAN7375, ΔAN8806 and wild-type strains under ionic liquids stimuli, free sphingoid bases were extracted as previously described in (107) and (108), with few modifications. Freshly harvested spores (10^6 conidia per ml) were inoculated in 100 ml of liquid **minimal medium** (described in Section 2.3) for 24 h at 30 ºC and agitation of 200 r.p.m. Ionic liquids $[C_{10}mim]Cl$, cholinium decanoate or $[P_{4\,4\,4\,12}]Cl$ were added to the cultures, at the concentration of 100 % of the determined MIC, and grown under the stress imposition for 1, 2 or 4 hours. Negative controls without the addition of ionic liquids were prepared. After each time point of incubation under stress, mycelia were recovered by vacuum filtration and immediately frozen in liquid nitrogen. All the samples were stored at -80 ºC until lyophilized. Approximately 80 mg of dried mycelia of each condition were grounded in a Tissue Lyser LT (Quiagen). Lipids were extracted in glass tubes with 5 ml of a solution containing 95 % ethanol/water/diethylether/pyridine/4.2 M ammonium hydroxide (15:15:5:1:0.018; by volume), sonicated for 5 min and then incubated for 15 min at 60 ºC. The extract was removed after centrifugation (1,620 x *g* for 5 min in a swing-bucket rotor) and the pellet extracted twice in the same manner. The lipid extracts were dried under a nitrogen flow. For methanolysis the dried extracts were resuspended in 5 ml of a solution containing methanol/ethanol/butanol/40 % methylamine in water (4:3:1:4, by volume) and incubated at 52 ºC for 30 min to ensure the deacylation of lipids. The resulting extracts were first dried under a nitrogen flow, then resuspended in 3 ml of methanol/chloroform (2:1, by volume) and to separate sphingoid bases to the organic layer 1 ml each of chloroform and alkaline solution (NH_4OH in water, pH 9.0) were added. The mixture was centrifuged (1,620 x *g* for 5 min in a swing-bucket

rotor) and the aqueous phase discarded. The organic phase was washed three times with 1 ml each of chloroform and alkaline solution, then dried under nitrogen flow. To perform alkaline hydrolysis the dried extracts were resuspended in 3 ml of 0.1 M KOH in methanol/chloroform (2:1, by volume) and incubated at 30 ºC for 1 hour to break down cellular acylglycerolipids and phospholipids. After incubation, 1 ml each of chloroform and alkaline solution were added and the mixture centrifuged (1,620 x *g* for 5 min in a swing-bucket rotor). The aqueous phase was discarded and the organic phase was washed three times in the same way, then dried under nitrogen flow and resuspended in methanol for further analysis of sphingoid bases by liquid chromatography.

2.8 High performance liquid chromatography analysis

For the analysis of sphingoid bases by high performance liquid chromatography (HPLC), it was necessary to perform a pre-column derivatisation with *o*-phthalaldehyde. The derivatisation reagent was prepared by dissolving 5 mg o-phthalaldehyde in 100 µl of methanol and 5 µl of β-mercaptoethanol, by mixing and sonicating. After complete dissolution, 9.9 ml of 3 % borate buffer (pH 10.5) was added and the solution stored at 4 ºC in the dark (stable for 4/5 days). Before the analysis, the sphingoid bases were derivatised by adding 25 µl of derivatisation solution to 200 µl of lipid samples in methanol, and incubated for 30 min at room temperature. The derivatised sphingoid bases were chromatographically separated using an Acquity UPLC System (Waters) with a fluorescence detector (acquisition with an energy gain of 1000), cooling auto-sampler, and column oven. A Symmetry® C18 reverse phase column (250 × 4.6 mm), packed with end-capped particles (5 µm, pore size 100 Å) was used at 40 °C. Data were acquired using Empower 2 software, 2006 (Waters Corporation). Sample injections of 10 µl were made using a 50 µl loop operated in partial loop mode. The mobile phase, at a flow rate of 1 ml min^{-1}, consisted of 90 % methanol. Each sample was run for 30 min and after each run the column was washed with water. Phytosphingosine, sphingosine and dihydrosphingosine standards eluted at 7.5, 10.55 and 13.7 min, respectively.

2.9 Determination of susceptibility to antifungal drugs

The susceptibility assays to antifungal drugs were performed by a colorimetric method using the MTT dye. The tested drugs include itraconazole, fluconazole, amphotericin B, flucytosine and terbinafine (all from Sigma-Aldrich); their stock solutions were prepared by dissolving the antifungal drugs in DMSO to a final concentration of 1 $mg \cdot ml^{-1}$. The tests were performed in 96-well microtitre plate and for each antifungal drug three biological replicates were prepared. Serial dilutions of the antifungal agents were made in RPMI 160 medium (Section 2.3) in order to have in each well 100 µl of antifungal drug with twice the final concentration, using a broth microdilution method according to NCCLS guidelines (109). The final concentration of the antifungal drugs ranged from 0.004 to 16.0 $mg \cdot l^{-1}$ for itraconazole, from 0.031 to 256.0 $mg \cdot l^{-1}$ for fluconazole, from 0.016 to 64.0 $mg \cdot l^{-1}$ for amphotericin B, from 0.031 to 128.0 $mg \cdot l^{-1}$ for flucytosine and from 0.0005 to

2.0 $mg \cdot l^{-1}$ for terbinafine. Fungal conidia of each strain were diluted in RPMI-160 medium to obtain a suspension with a final concentration of 2 x 10^6 conidia per ml. Each well of the microtitre plate was inoculated with 100 µl of spore suspension, which give the required final drug concentration and inoculum density of 10^6 conidia per ml. The plates were incubated for 24 h at 37 ºC, without agitation. After incubation, 25 µl MTT solution (5 mg of MTT per 1 ml of 0.85 % (w/v) NaCl solution) was added to each well and incubated for more 4 h at 37 ºC. After, the content of each well was removed carefully and 200 µl of isopropanol containing 5 % 1 M HCl was added to extract the dye. After 15 min of incubation at room temperature and gentle mixing with a micropipette, 100 µl were transferred to a new plate and the absorbance measured at 570 nm (A_{570nm}) using an Infinite M2000 Spectrophotometer (Tecan). The percentage of MTT conversion to its formazan derivate was calculated based on the following equation: [(A_{570nm} well containing drug – background A_{570nm})/(A_{570nm} well without drug – background A_{570nm})] x 100. The test was carried out in triplicates and the results were analysed by nonlinear regression analysis by using a four parameter logistic model (sigmoid curve with variable slope), which is described by the following equation: $E = 100/[1+(D^{HillSlope})/(EC_{50}^{HillSlope})]$, where E is the relative A_{570nm}, D is the drug concentration and EC_{50} is the drug concentration producing 50 % of the effect. The differences between the best-fit values of the concentration effect curves for all strains were analysed by one-way ANOVA analysis of variance with Dunnett's test, statistical significance was considered when P values were < 0.05. Analysis was carried out using GraphPad 6.01 software.

CHAPTER 3 – Results

3.1 Gene identification for target deletion 26

3.2 Confirmation of gene deletion 27

3.3 Sphingoid bases chromatographic profile of mutant strains 30

3.4 Ionic liquids minimal inhibitory concentration 32

3.5 Growth ability in presence of ionic liquids 32

3.6 Analysis of sphingoid base accumulation induced by ionic liquids 35

3.7 Susceptibility to antifungal drugs 38

3.1 Gene identification for target deletion

To identify *A. nidulans* putative genes coding for sphingolipid Δ4-desaturase, sphingolipid Δ8-desaturase, C9-methyltransferase and glucosylceramide synthase to later construct deletion cassettes, sequences of previously characterized proteins from different organisms were used as queries in protein-protein BLAST (Basic Local Alignment Search Tool) analysis.

BLAST analysis using the dihydroceramide Δ4-desaturase sequence from *Schizosaccharomyces pombe* (encoded by the *dsd1* gene) (110) revealed a hypothetical protein encoded by the **AN4405** gene (e-value = 1e-130, 93.0 % query coverage and 54.0 % identity), consistent with the predicted functions described in the *Aspergillus* Genome Database. The AN4405 gene model is located at chromosome III and comprises 1,381 nucleotides with two introns from 211 to 273 and 553 to 613; the open reading frame (ORF) contains 1,257 nucleotides encoding 418 amino acids (47.2 kDa protein). BLAST analysis with sphingolipid Δ8-desaturase protein sequence from the pathogenic yeast *C. albicans* (*SLD1* gene) (75), revealed a hypothetical protein encoded by the **AN4592** gene (e-value = 0.0, 96.0 % query coverage and 47.0 % identity). The AN4592 gene model is located in chromosome III and comprises 1,693 nucleotides with one intron from 189 to 243; the ORF contains 1,638 nucleotides encoding 545 amino acids (63.2 kDa protein).

BLAST analysis with the protein sequence of sphingolipid C9-methyltransferase from *C. albicans* (encoded by the *SMT1* gene) (111), revealed two putative proteins encoded by **AN5688** (e-value = 0.0, 96.0 % query coverage and 62.0 % identity) and **AN7375** (e-value = 0.0, 95.0 % query coverage and 56.0 % identity) genes. The alignment of these two putative genes showed e-value = 6e-69 and 67 % identity, which suggests that they are paralogues. The AN5688 gene model is located at chromosome V, comprises 1,759 nucleotides with three introns from 106 to 206, 694 to 746 and 1499 to 1549; the ORF contains 1,554 nucleotides encoding 517 amino acids (58.2 kDa). The AN7375 gene model is located at chromosome IV, comprises 1,689 nucleotides with three introns from 118 to 168, 1293 to 1339 and 1449 to 1506; the ORF contains 1,533 nucleotides encoding 510 amino acids (57.7 kDa). This result is supported by previous phylogenetic profile analysis that revealed the existence of two candidate C9-methyltransferase genes in *A. nidulans* (72).

The identification of the putative glucosylceramide synthase was based on the protein sequence from *C. albicans* (encoded by the *HSX11* gene) (112). The BLAST analysis revealed a hypothetical protein encoded by **AN8806** gene (e-value = 4e-85, 98.0 % query coverage and 32.0 % identity). The AN8806 gene model is located at chromosome III, comprises 1,710 nucleotides with one intron from 147 to 197; the ORF contains 1,659 nucleotides encoding 552 amino acids (62.0 kDa)

3.2 Confirmation of gene deletion

Aspergillus nidulans gene disruption was performed by replacement of target genes with a deletion cassette containing *pyr*G gene from *A. fumigatus* (*pyrG*^{Af}), and the transformed colonies were selected by their ability to grow in the absence of uracil and uridine. Homologous recombination was confirmed by diagnostic PCR and digestion of its products with different restriction enzymes that have differential recognition of *pyrG*^{Af} and AN4405, AN4592, AN5688, AN7375 and AN8806 sequences.

The PCR products of ΔAN4405 colonies possess 3,708 bp while the wild-type has 3,436 bp. The HpaI enzyme has two recognition sites on AN4405 sequence, thus digestion of the fragment containing the AN4405 gene produces three fragments with 2,017, 1,326 and 93 bp. This enzyme does not have recognition sites in the *pyrG*^{Af} sequence (Figure 3.1A). The resulting undigested and digested PCR products were run on an agarose gel (Figure 3.1a). The expected 3,436 bp size band was amplified from the wild-type DNA, while in the ΔAN4405 strain a larger size band is present. The digestion of the amplified fragment from the wild-type originated two bands with approximately 1,400 and 2,000 bp, whereas the 93 bp fragment cannot be visualised in the gel due to its small size. In the ΔAN4405 strain this pattern was not observed. Instead, we could observe a single band near 4,000 bp.

The amplified fragment from ΔAN4592 colonies possesses 3,845 bp while the wild-type has 3,844 bp. The restriction enzyme ApaI has no recognition sites on the AN4592 sequence. However, it has two recognition sites on the *pyrG*^{Af} sequence producing three distinct sized fragments – 1,929, 1,693 and 222 bp (Figure 3.1B). In the agarose gel, bands from the undigested PCR products from wild-type and ΔAN4592 strain have approximately the same size. The digestion of ΔAN4592 fragments with ApaI generated two bands between 1,400 and 2,000 bp. However the smaller band, corresponding to 222 bp, could not be observed probably due to its size. In the wild-type digested product, it was possible to observe a single band at 4,000 bp (Figure 3.1b).

The amplified fragments from ΔAN5688 and wild-type colonies have 3,766 and 3,798 bp, respectively. The digestion with BglII produces two fragments with 2,565 and 1,233 on AN5688 gene sequence; however, this enzyme does not possess a recognition site in the *pyrG*^{Af} sequence (Figure 3.2A). In the agarose gel it was possible to observe that the undigested PCR products are of the same size, nearly 4,000 bp. Digestion of wild-type fragments with BglII enzyme originates two bands, one near to 2,500 bp and another slightly above 1,000 bp. In the ΔAN5688 strain after the digestion, this pattern was not observed; instead one single band near to 4,000 bp could be seen (Figure 3.2a).

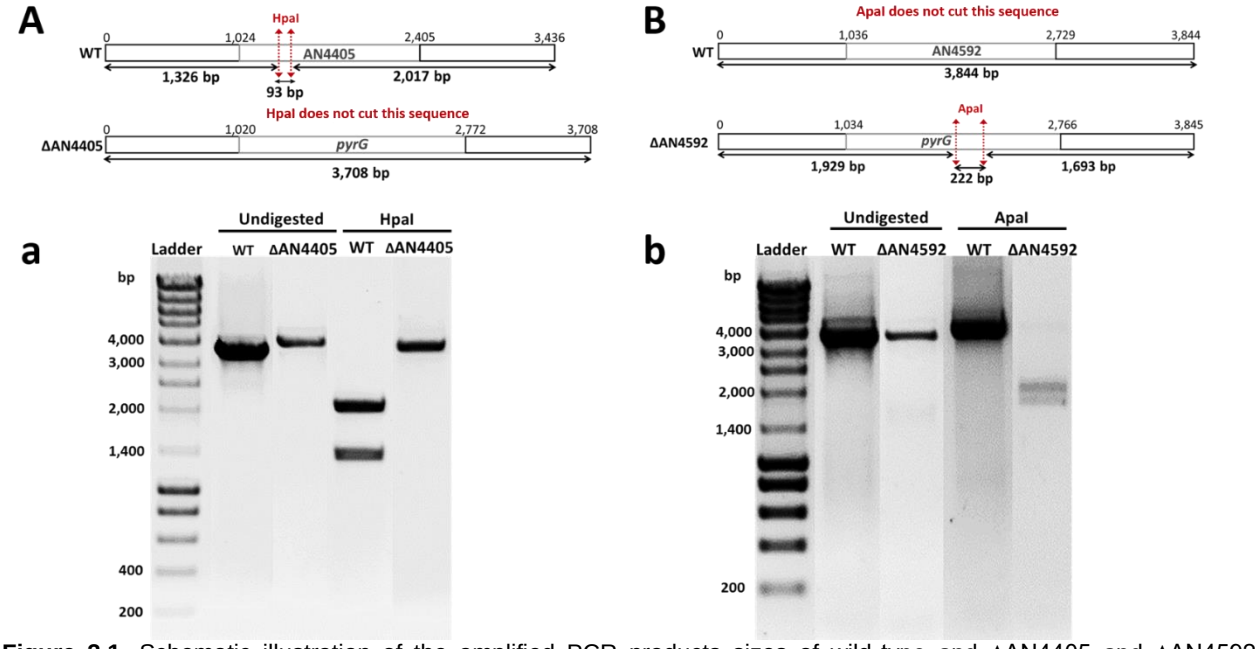

Figure 3.1. Schematic illustration of the amplified PCR products sizes of wild-type and ΔAN4405 and ΔAN4592 candidate colonies, and their respective digestion products with HpaI and ApaI enzymes (restriction sites are shown by red arrows, respectively A and B). The resulting undigested and digested PCR products were run on an agarose gel and the differential fragments sizes lead to the identification of colonies with gene disruption (a and b). The sizes of the obtained bands were compared to NZYDNA Ladder III.

The amplified fragments from ΔAN7375 colonies and wild-type have 3,752 and 3,756 bp, respectively. The BglII enzyme has one recognition site on the AN7375 sequence which produces two fragments with 2,547 and 1,209 bp, however, this enzyme does not have recognition sites on the *pyrG*^{Af} sequence (Figure 3.2B). The undigested PCR products from wild-type and ΔAN7375 that were run on an agarose gel displayed bands of the same size, slightly above 3,000 bp. The digested wild-type fragments with BglII originated two bands, one below 3,000 bp and another one between 1,400 and 1,000 bp. In the digested ΔAN7375 strain only a single band was observed, which is indicative that the enzyme does not possess any recognition site in this construct (Figure 3.2b).

The PCR products of ΔAN8806 colonies and of wild-type have 3,692 and 3,782 bp, respectively. The used restriction enzyme NcoI has one recognition site on the AN8806 gene sequence, which produces two fragments with 1,958 and 1,824 bp and no recognition sites on the *pyrG*^{Af} sequence (Figure 3.2C). In the agarose gel, it is possible to observe two bands of approximately the same size that correspond to the undigested PCR products from wild-type and ΔAN8806 strain. The digested wild-type fragments appeared as one intense band slightly above 2,000 bp, probably because the two fragments have very similar sizes which are observed as a unique intense band. The digested ΔAN5688 strain fragments were observed as one single band near 4,000 bp.

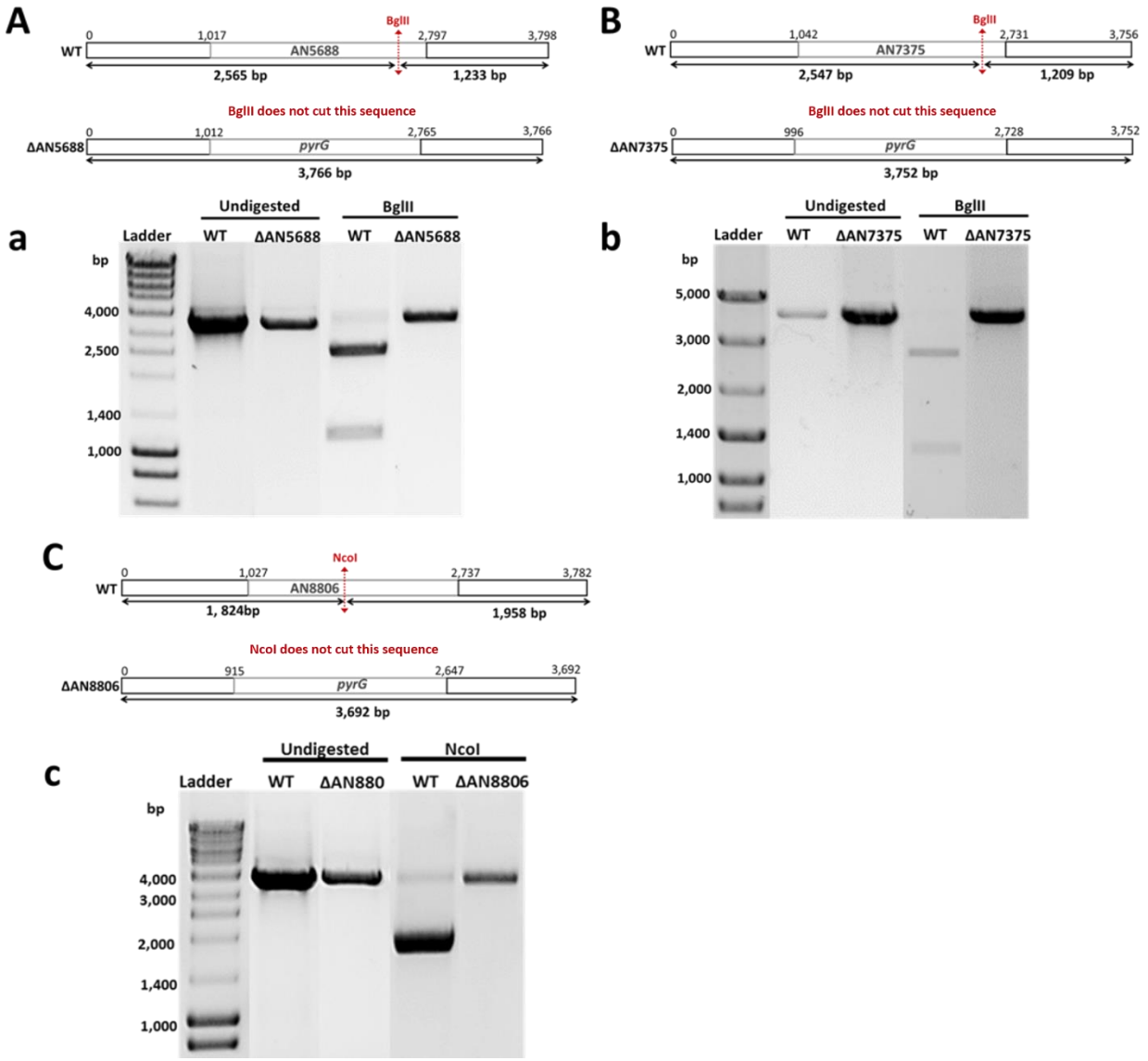

Figure 3.2. Schematic illustration of the band sizes of the amplified PCR products from ΔAN5688, AN7375 and ΔAN8806 candidate colonies and wild-type, and their respective digestion with BglII (A and B) and NcoI (C) enzymes, whose restriction sites are shown by red arrows. The resulting undigested and digested PCR products were run on an agarose gel and the differential fragments sizes lead to identification of colonies with gene disruption (a, b and c). The sizes of obtained bands were compared to NZYDNA Ladder III (a and c) and NZYDNA Ladder VIII (b).

3.3 Sphingoid bases chromatographic profile of mutant strains

To evaluate the pattern of accumulation of sphingoid bases in the wild-type and the mutant strains high performance liquid chromatography (HPLC) analyses of the corresponding lipid extracts of cultures grown in liquid minimal medium for 24 hours without any stress imposition were performed (Figure 3.3). The identification of the peaks was performed taking into account the retention time of the used standards, phytosphingosine (PHS), sphingosine (SPH) and dihydrosphingosine (DHS). Nevertheless, it is possible that similar compounds are not separated, being eluted at the same peak.

We have observed that each mutant strain present a distinct accumulation profile of sphingoid bases. In the wild-type a peak corresponding to PHS was clearly distinguished, yet a minor peak corresponding to an unknown compound with a retention time at 9.55 min was also observed (compound **x**). The ΔAN4405 strain apparently accumulated PHS and DHS (Figure 3.3B). On the other hand, ΔAN4592 strain accumulated the known sphingoid bases, PHS and SPH (Figure 3.3C). Major accumulation of PHS was observed for both ΔAN5688 and ΔAN7375 strains, together with accumulation of DHS (Figure 3.3D and E). The ΔAN8806 mutant notably accumulates PHS, DHS and, to a lower extent, also SPH (Figure 3.3F) together with major accumulation of the unknown compound **x** (retention time at 9.55 min) (Figure 3.3F). In addition, all the mutant strains with exception of ΔAN4592 seem to slightly accumulate an unknown compound with retention time at 11.55 min (compound **y**). The presence of unknown compounds between the retention times of 3.5 and 5.2 min was observed for all strains (Figure 3.3), within these the compound **α** (retention time at 3.8 min) was the most interesting, especially for ΔAN4405 (Figure 3.3B).

Additionally, it was observed that ΔAN4405 and ΔAN4592 growth in liquid medium was hindered compared to the remaining strains (data not shown).

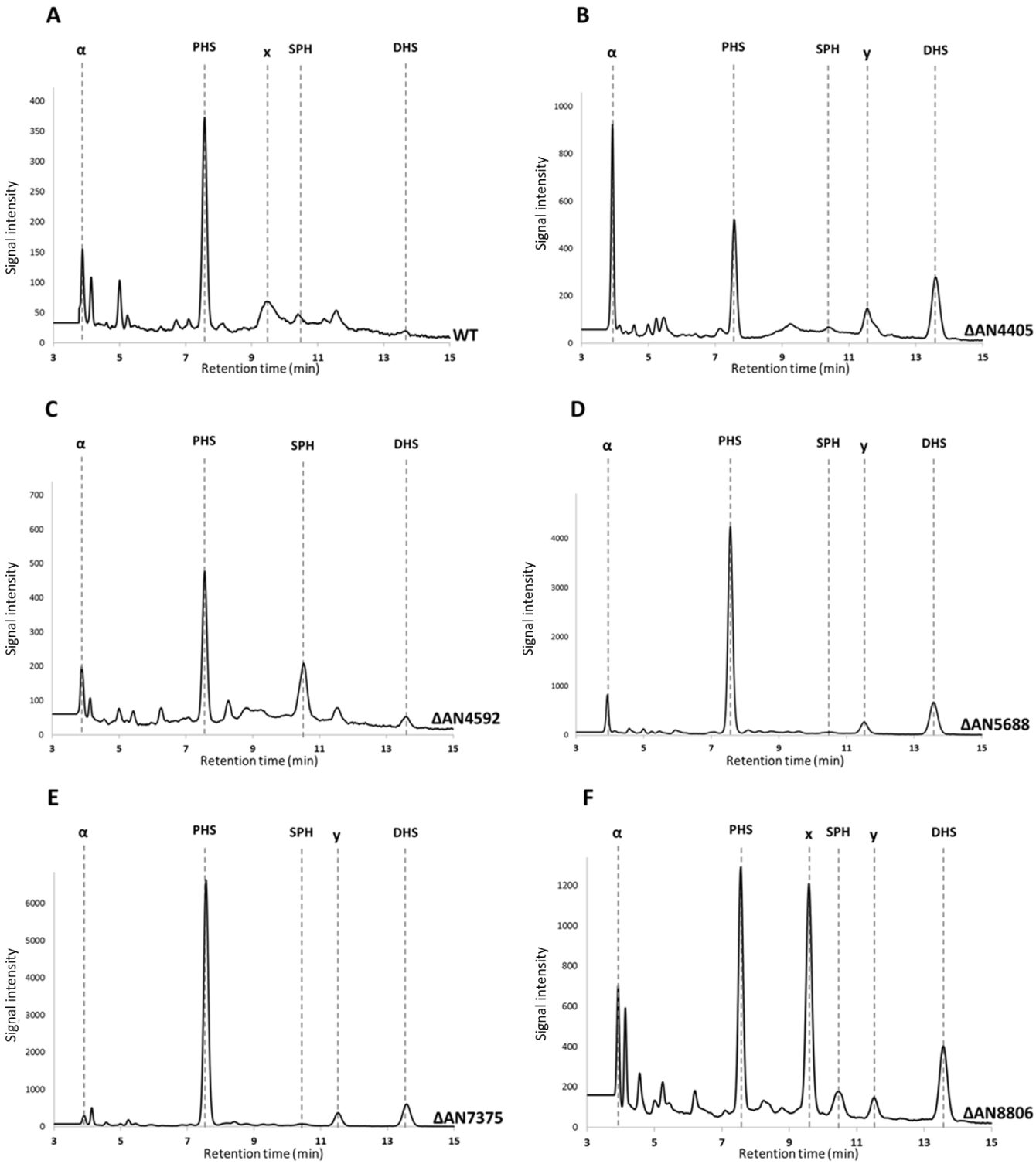

Figure 3.3. Chromatographic profile (HPLC) of sphingoid bases from the lipid extract of mycelia of *A. nidulans* wild-type strain (A) and mutant strains and mutant strains ΔAN4405 (B), ΔAN4592 (C), ΔAN5688 (D), ΔAN7375 (E) and ΔAN8806 (F) after 24 hours of growth in minimal medium without stress imposition. PHS = phytosphingosine; SPH = sphingosine; DHS = dihydrosphingosine; α = unknown compound with retention time at 3.8 min; x = unknown compound with retention time at 9.55 min; y = unknown compound with retention time at 11.55 min. **The scale of signal intensity is different in each chromatogram**.

3.4 Ionic liquids minimal inhibitory concentration

The minimal inhibitory concentration (MIC) of each ionic liquid (IL), namely [C_{10}mim]Cl, [$P_{4\,4\,4\,12}$]Cl and cholinium decanoate, against the glucosylceramide (GlcCer) biosynthetic pathway gene deletion strains ΔAN4405, ΔAN4592, ΔAN5688, ΔAN7375 and ΔAN8806, are represented in Table 3.1. Some differences between wild-type and the mutants could be observed. The ΔAN4405 and ΔAN4592 strains compared to the wild-type showed higher susceptibility to [C_{10}mim]Cl than the other mutants, which displayed an apparently increased tolerance. Regarding cholinium decanoate, ΔAN4405, ΔAN4592 and ΔAN8806 strains were more sensitive, while the remaining mutants showed lower susceptibility to this ionic liquid. [$P_{4\,4\,4\,12}$]Cl seems to have similar effect on all mutant and wild-type strains.

The induction of chemical stress with these ionic liquids in fungi, relied on the use of 100 % of the determined MIC. Since the time of incubation under stress is very short (maximum 4 hours), the ionic liquids are unable to kill the fungus, yet they induce a sufficiently strong stress signal to activate a major response.

T**able 3.1** Values of obtained minimal inhibitory concentrations of the three tested ionic liquids against *Aspergillus nidulans* mutants and wild-type strains, after growth in liquid minimal medium for 6 days.

	Minimal inhibitory concentration (mM)		
Strains	**[C_{10}mim]Cl**	**[$P_{4\,4\,4\,12}$]Cl**	**Cholinium decanoate**
WT	0.15	0.012	3.0
ΔAN4405	0.10	0.013	2.7
ΔAN4592	0.11	0.013	2.4
ΔAN5688	0.19	0.012	3.4
ΔAN7375	0.21	0.010	3.3
ΔAN8806	0.17	0.011	2.5

3.5 Growth ability in presence of ionic liquids

The growth ability of GlcCer biosynthetic pathway mutants in presence of [C_{10}mim]Cl, [$P_{4\,4\,4\,12}$] or cholinium decanoate was determined by their radial growth on solid minimal medium containing the tested ionic liquids. The inhibition caused by the ionic liquid was determined comparing the colony size (*i.e.* diameter) grown in medium with the ionic liquid and in control media. The statistical significance of the difference of inhibition between each mutant colony and wild-type colony in same condition was analysed by one-way ANOVA.

A preliminary screen was performed in order to define the ionic liquid concentration range in solid medium and in all depicted Figures 3.4, 3.5 and 3.6, we only represent the ionic liquid concentration where

a noticeable effect was observed. In medium containing 0.15 mM of [C_{10}mim]Cl, 0.025 Mm of [$P_{4\,4\,4\,12}$]Cl or 1.5 mM cholinium decanoate, none of the strains was able to germinate (data not shown).

The hyphal growth in minimal medium without the addition of the ionic liquids (controls) of ΔAN4405, ΔAN4592 and ΔAN8806 strains was reduced compared to wild-type and also to ΔAN5688 and ΔAN7375 strains (Figure 3.4A).

Although not visually noticeable (Figure 3.4A), it is possible to observe through growth inhibition values that the ΔAN4405, ΔAN4592 and ΔAN8806 strains were more resistant to [C_{10}mim]Cl. In fact, the lower concentrations herein tested seem to have stimulated growth (Figure 3.4B top). The ΔAN7375 strain was slightly more sensitive to this ionic liquid in one of the tested conditions, while the ΔAN5688 was notably more resistant (Figure 3.4A and 3.4B bottom).

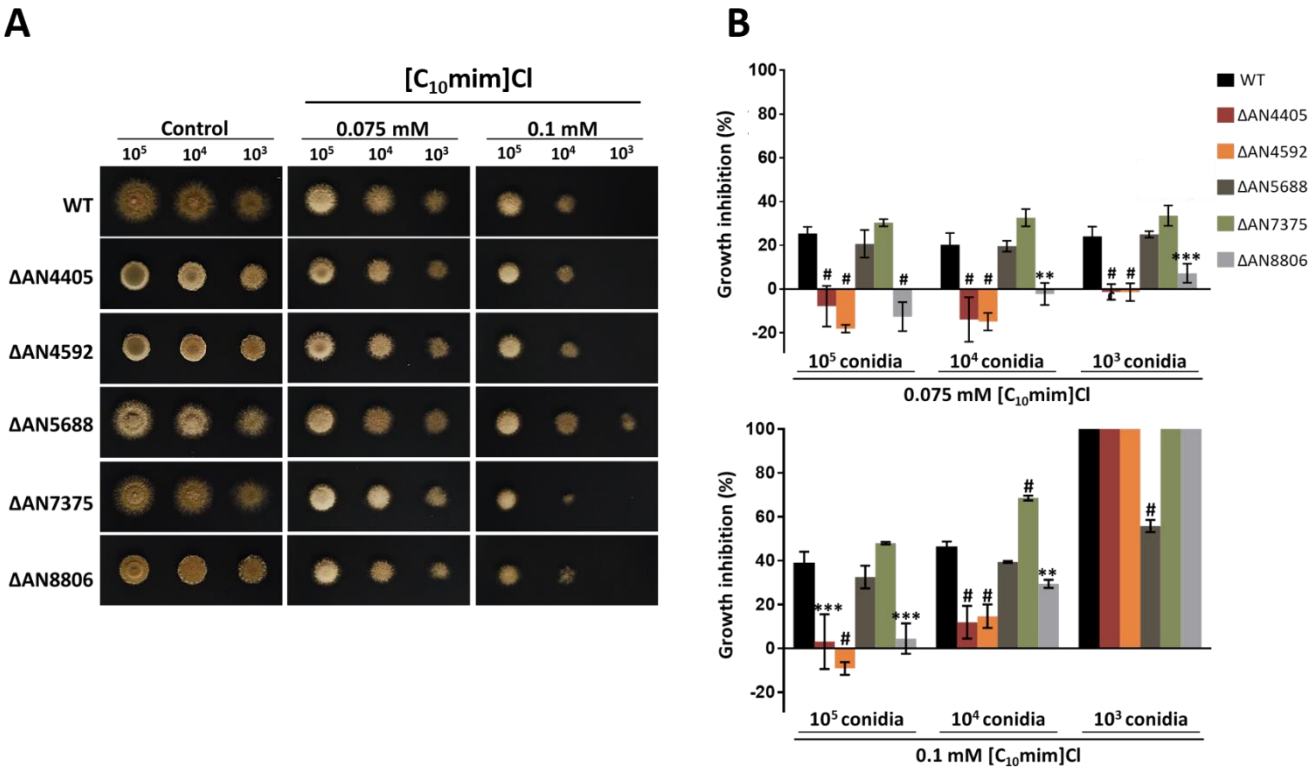

Figure 3.4. Susceptibility of GlcCer biosynthetic pathway mutants to [C_{10}mim]Cl in solid medium. The indicated amount of conidia was point inoculated in minimal medium supplemented or not (control) with 0.075 or 0.1 mM of [C_{10}mim]Cl and grown for 48h at 30 ºC (A). The growth inhibition caused by the ionic liquid was determined through growth diameter measurements. The results are the average of three replicates ± SD. The variance was analysed by one-way ANOVA and the significant differences in inhibition of each mutant compared to the wild-type for the same condition represented, *****P ≤ 0.05, ******P ≤ 0.01, *******P ≤ 0.001 and $^{\#}$P ≤ 0.0001, (B).

Interestingly, all five mutants showed increased resistance to phosphonium-based IL, [$P_{4\,4\,4\,12}$]Cl (Figure 3.5A), with similar levels of growth in all conditions (Figure 3.5B). In the presence of ionic liquids, the ΔAN4405 and ΔAN4592 strains exhibited an approximately 27-39% reduction in radial growth and the

ΔAN8806 between 45-56%. The ΔAN5688 and ΔAN7375 exhibited a slight sensitivity to [$P_{4\,4\,4\,12}$]Cl comparatively to the other three mutants, showing 59-69% of reduction in growth. When grown on medium containing 0.025 Mm of [$P_{4\,4\,4\,12}$]Cl none of the strains was able to germinate (data not shown).

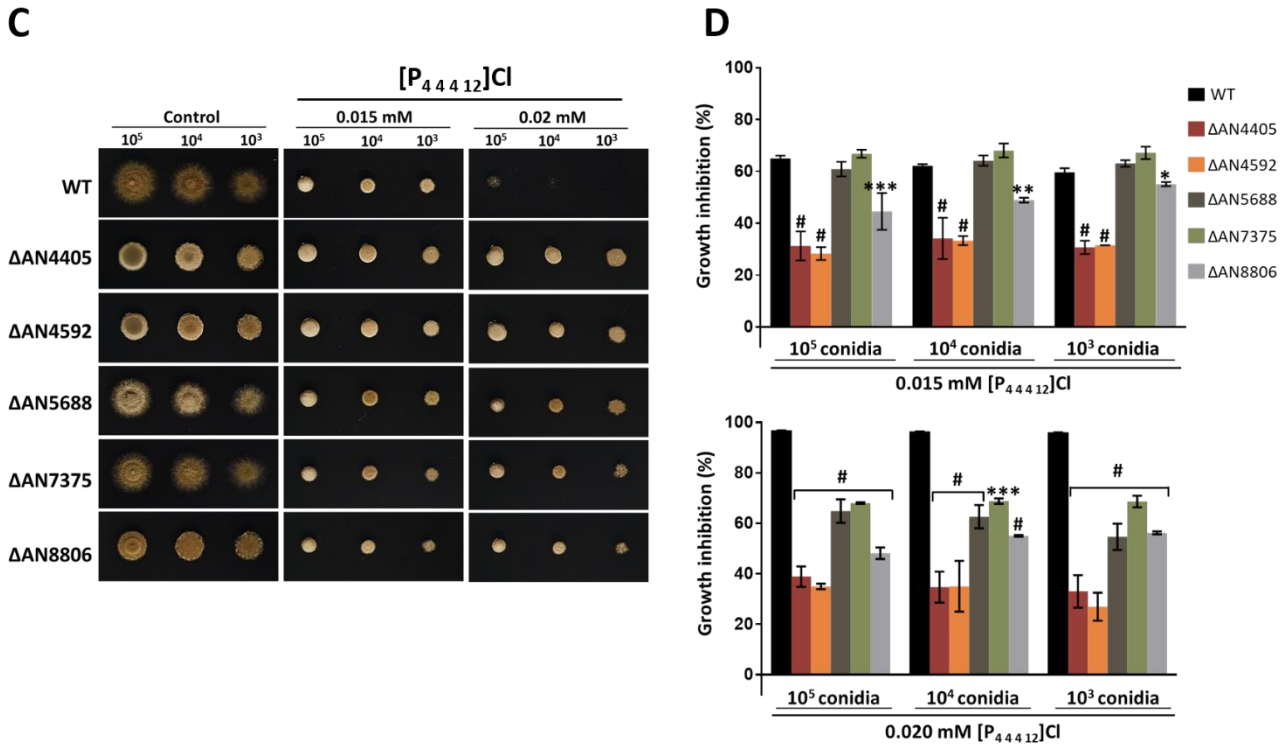

Figure 3.5. Susceptibility of GlcCer biosynthetic pathway mutants to [$P_{4\,4\,4\,12}$]Cl in solid medium. The indicated amount of conidia was point inoculated in minimal medium supplemented or not (control) with 0.015 or 0.020 mM of [$P_{4\,4\,4\,12}$]Cl and grown for 48h at 30 ºC (A). The growth inhibition caused by the ionic liquid was determined through growth diameter measurements. The results are the average of three replicates ± SD. The variance was analysed by one-way ANOVA and the significant differences in inhibition of each mutant compared to the wild-type for the same condition represented, *****P ≤ 0.05, ******P ≤ 0.01, *******P ≤ 0.001 and #P ≤ 0.0001, (B).

The hyphal growth and differentiation was also analysed in the presence of cholinium decanoate (Figure 3.6). Notably, the strain lacking the AN4592 gene demonstrated high susceptibility to this ionic liquid (Figure 3.6A). Also, the ΔAN8806 strain was slightly sensitive to cholinium decanoate (Figure 3.6B, bottom). The remaining mutants displayed lower growth inhibition when incubated with this ionic liquid compared to the wild-type strain (Figure 3.6B).

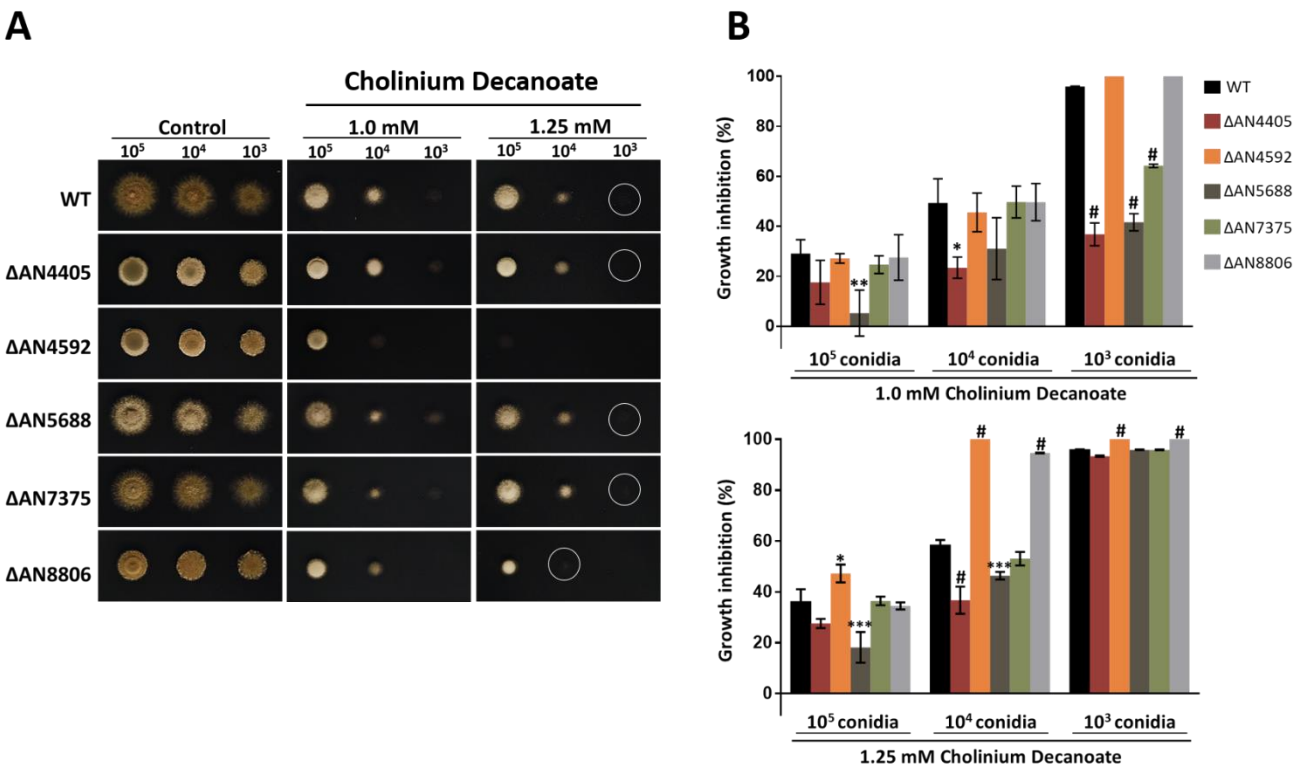

Figure 3.6. Susceptibility of GlcCer biosynthetic pathway mutants to cholinium decanoate in solid medium. The indicated amount of conidia was point inoculated in minimal medium supplemented or not (control) with 1.0 or 1.25 mM of cholinium decanoate and grown for 48h at 30 ºC, the withe circles mark the colonies where slight growth was observed (A). The growth inhibition caused by the ionic liquid was determined through growth diameter measurements. The results are the average of three replicates ± SD. The variance was analysed by one-way ANOVA and the significant differences in inhibition of each mutant compared to the wild-type for the same condition represented, *****P ≤ 0.05, ******P ≤ 0.01, *******P ≤ 0.001 and #P ≤ 0.0001, (B).

3.6 Analysis of sphingoid base accumulation induced by ionic liquids

To further investigate the accumulation of sphingoid bases upon an ionic liquid stress, the mutants strains and the wild-type strain were exposed to $[C_{10}mim]Cl$, cholinium decanoate or $[P_{4\,4\,4\,12}]Cl$ for 1, 2 and 4 hours, and the ensuing fungal biomass used for lipid extraction. A control condition, without stress imposition, was also prepared for each time point. Sphingoid bases from the extracted lipid fraction were derivatised with *o*-phthalaldehyde and further analysed by HPLC. A more pronounced response through accumulation of compounds was observed after 4 hours of exposition to ILs. The identification of the peaks was performed taking into account the retention time of the used standards, phytosphingosine (PHS), sphingosine (SPH) and dihydrosphingosine (DHS). However, it is possible that similar compounds are not separated, being eluted at the same peak.

In the control condition, after 4 hours of incubation without stress imposition, all the strains slightly accumulated an unknown compound with a retention time of 11.15 min (Figure 3.7A and B, compound **z**).

Furthermore, the wild-type, ΔAN4405, ΔAN4592 and ΔAN8806 strains slightly accumulated PHS, while the ΔAN5688 and ΔAN7375 strains accumulated a greater amount of this sphingoid base (Figure 3.7). Also, accumulation of DHS was observed for all the mutants, except for ΔAN4592 strain (Figure 3.7). A small unknown peak with retention time 11.55 min (Figure 3.7B, compound **y**) was observed for ΔAN5688 and ΔAN7375. The ΔAN4592 and ΔAN8806 strains slightly accumulated SPH, and the last one also apparently accumulated a great amount of an unknown compound with a retention time at 9.55 min (Figure 3.7B, compound **x**). Moreover, all the strains, most notably the ΔAN4405, accumulated a great amount of an unknown compound with a retention time at 3.8 min (compound **α**).

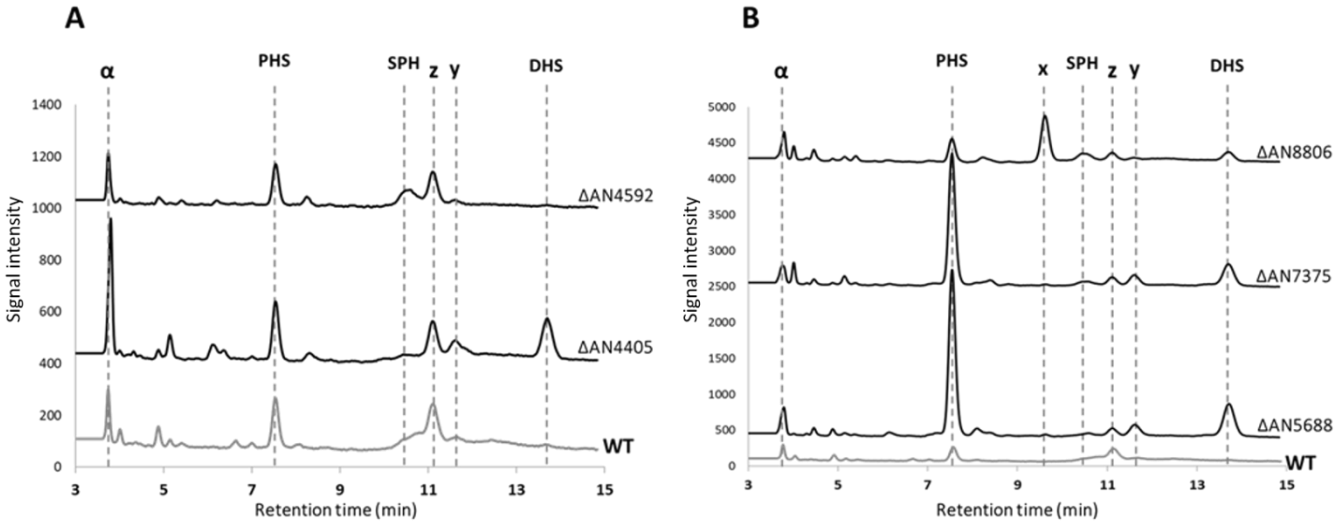

Figure 3.7. Chromatographic profile (HPLC) of sphingoid bases from the lipid extract of mycelia after 4 hours of incubation of *A. nidulans* wild-type strain and mutant strains in control media, without stress imposition: ΔAN4405 and ΔAN4592 (A); ΔAN5688, ΔAN7375 and ΔAN8806 (B). PHS = phytosphingosine; SPH = sphingosine; DHS = dihydrosphingosine; α = unknown compound with retention time at 3.8 min; x = unknown compound with retention time at 9.55 min; y = unknown compound with retention time at 11.55 min; z = unknown compound with retention time at 11.15 min. **The scale of signal intensity is different in each chromatogram.**

Fungal incubation with [C_{10}mim]Cl does not seem to have induced a noticeable accumulation of the known sphingoid bases, PHS or DHS (Figure 3.8 A and B) in any of the tested strains, with exception of wild-type and ΔAN4405 strains that apparently slightly accumulated PHS (Figure 3.8A). In fact, compared to the controls (cultures without stress imposition) a decrease of DHS amounts was observed in all mutants and a more pronounced decrease of PHS in ΔAN5688 and ΔAN7375 strains (Figure 3.8A), whereas the ΔAN4592 and ΔAN8806 strains retained PHS amount. Interestingly, this imidazolium-based IL induced the accumulation of an unknown compound, with a retention time of 8.0 min in all cultures. ΔAN7375 and ΔAN8806 showed an increased accumulation of the same compound (Figure 3.8, compound **i**). In the control condition none of the strains accumulated this unknown compound (Figure 3.7). Additionally, for ΔAN5688, ΔAN7375 and ΔAN8806 a smaller peak was observed with a retention time of 8.4 min

(Figure 3.8B, compound **ii**), this peak was not observed in the wild-type strain. Thus, this ionic liquid appears to be inducing the accumulation of distinctive sphingoid intermediates. The ΔAN8806 strain accumulated a similar amount of unknown compound **x** with retention time of 9.55 min (Figure 3.8B) after exposure to [C_{10}mim]Cl.

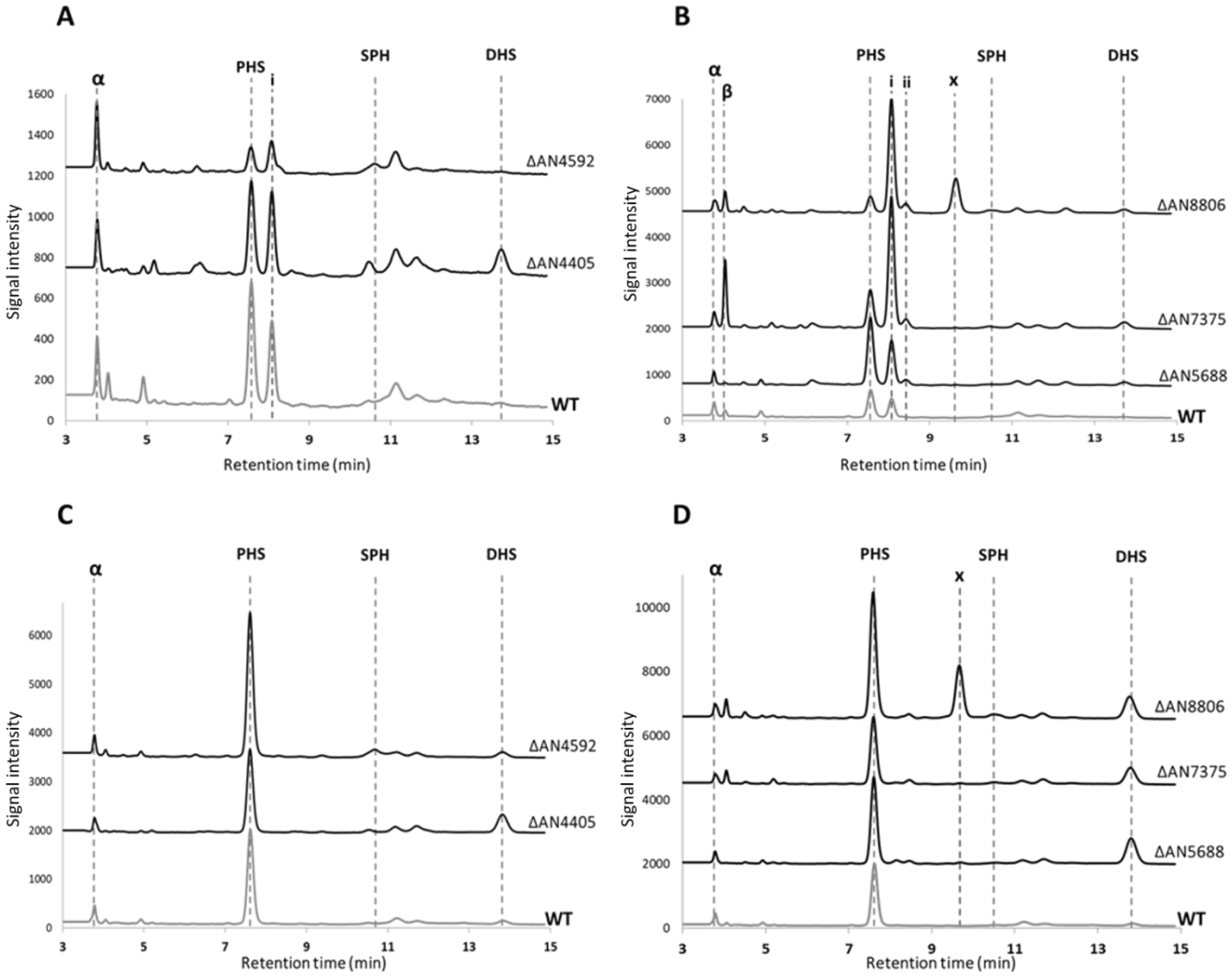

Figure 3.8. Chromatographic profile (HPLC) of sphingoid bases from the lipid extract of mycelia after 4 hours of incubation of *A. nidulans* wild-type strain and mutant strains in media supplemented with [C_{10}mim]Cl (A and B) or [$P_{4\ 4\ 4\ 12}$]Cl (C and D): ΔAN4405 and ΔAN4592 (A and C); ΔAN5688, ΔAN7375 and ΔAN8806 (B and D). PHS = phytosphingosine; SPH = sphingosine; DHS = dihydrosphingosine; α = unknown compound with retention time at 3.8 min; β = unknown compound with retention time at 4.1 min; i = unknown compound with retention time at 8.0 min; ii = unknown compound with retention time at 8.4 min; x = unknown compound with retention time at 9.55 min. **The scale of signal intensity is different in each chromatogram.**

An increased accumulation of PHS was induced by the phosphonium-based IL, most notably for wild-type, ΔAN4405, ΔAN4592 and ΔAN8806 (Figure 3.8C), compared to the control condition; just a slight increase in its amount was observed for the ΔAN5688 and ΔAN7375 (Figure 3.8D). In addition, all the strains

showed an increase in DHS amount, most pronounced for ΔAN8806 (Figure 3.8D). [$P_{4\,4\,4\,12}$]Cl apparently also induced a slight accumulation of SPH in the ΔAN4592 and ΔAN8806 strains (Figure 3.8D). Additionally, a great increase in the accumulation of the unknown compound with retention time of 9.55 min was observed for ΔAN8806 mutant (Figure 3.8, compound ***x***).

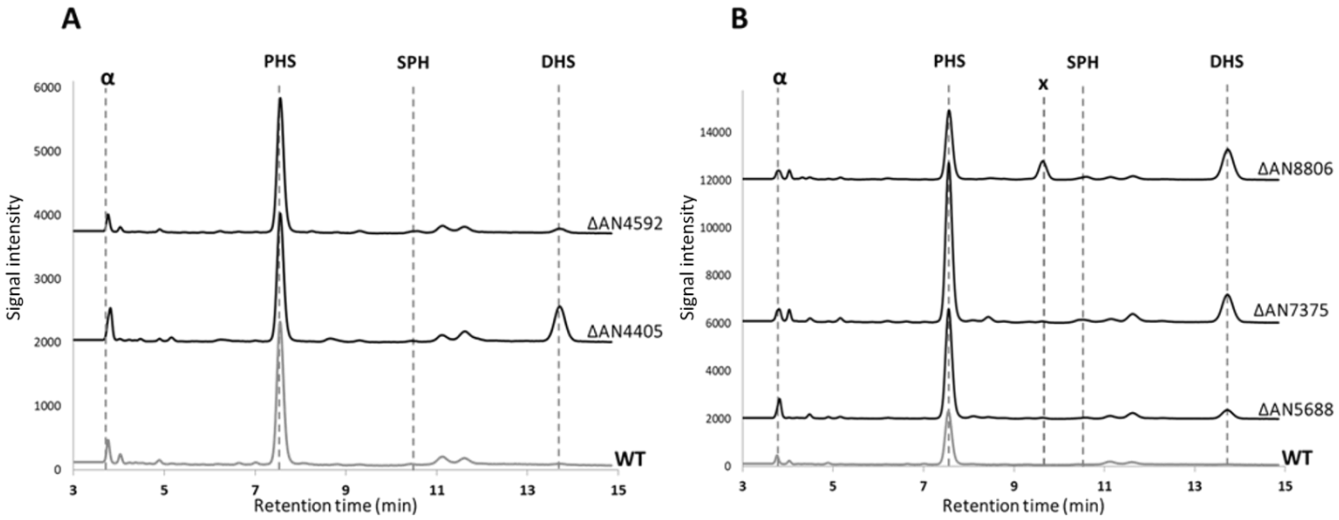

Figure 3.9. Chromatographic profile (HPLC) of sphingoid bases from the lipid extract of mycelia after 4 hours of incubation of *A. nidulans* wild-type strain and mutant strains in media supplemented with cholinium decanoate: ΔAN4405 and ΔAN4592 (A); ΔAN5688, ΔAN7375 and ΔAN8806 (B). PHS = phytosphingosine; SPH = sphingosine; DHS = dihydrosphingosine; α = unknown compound with retention time at 3.8 min; x = unknown compound with retention time at 9.55 min. **The scale of signal intensity is different in each chromatogram.**

The cholinium decanoate apparently induced a large accumulation of PHS peak (Figure 3.9A) in all the strains. Additionally, for ΔAN4405, ΔAN7375 and ΔAN8806 strains, accumulation of DHS was observed, whereas in ΔAN5688 a slight decrease in DHS accumulation was observed instead (Figure 3.9B). The ΔAN8806 accumulated a similar amount of an unknown compound with retention time of 9.55 min (compound ***x***) after exposure to this ionic liquid.

3.7 Susceptibility to antifungal drugs

The susceptibility of the *A. nidulans* mutants to antifungal drugs was tested by a colorimetric method using the MTT dye. The concentration-effect curves were obtained using a four parameter logistic model and the obtained EC_{50} (drug concentration producing 50 % of the effect) values compared for each strain. The statistical significance of the difference of EC_{50} values between each mutant and wild-type was analysed by one-way ANOVA test.

As depicted in Figure 3.10, the mutants showed varied susceptibilities to the different antifungal agents. The ΔAN5688 and ΔAN7375 strains were less susceptible to itraconazole and fluconazole, while

the remaining mutants seem to be more susceptible to fluconazole (Figures 3.10A and B). The ΔAN4405 and ΔAN8806 strains required exposure to a higher dose of amphotericin B to show the same effect as the wild-type (Figure 3.10C). All the mutants, with the exception of ΔAN8806, were more resistant to terbinafine effect (Figure 3.10D) and the ΔAN4405, ΔAN4592, ΔAN5688 and ΔAN8806 strains were more sensitive to flucytosine (Figure 3.10E).

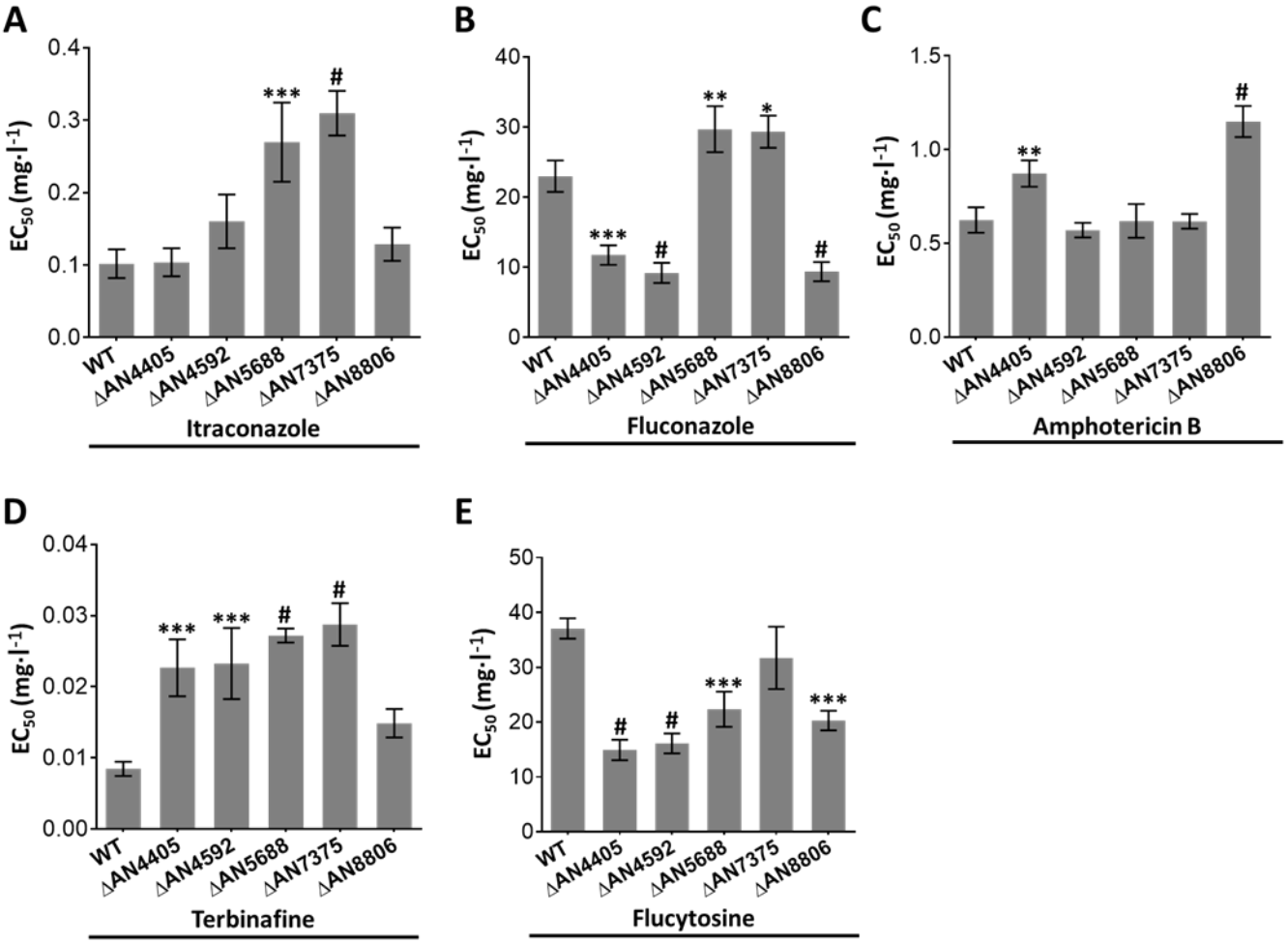

Figure 3.10. Susceptibility of *Aspergillus nidulans* mutants to antifungal drugs. The best-fit EC_{50} values ± SD for itraconazole (A), fluconazole (B), amphotericin B (C), terbinafine (D) and flucytosine (E) were obtained by nonlinear regression analysis. The variance was analysed by one-way ANOVA and the significant differences for each mutant when compared to the wild-type represented, *****P ≤ 0.05, ******P ≤ 0.01 *******P ≤ 0.001 and $^{\#}$P ≤ 0.0001.

CHAPTER 4 – Discussion and Future Perspectives

This work aimed at studying the impact of sphingolipid biosynthesis in stress responses of *Aspergillus nidulans*. It has been previously observed by our team that stimuli of some families of ionic liquids affects the sphingolipid biosynthetic pathway, leading to accumulation of both known and unknown sphingoid bases (79). It was hypothesised that these unknown accumulated compounds may be the intermediates of the glucosylceramide (GlcCer) biosynthetic pathway and that their accumulation relates to their involvement in the activation of stress response pathways, mainly the cell way integrity pathway, in *A. nidulans*. To further study this hypothesis, we identified putative genes of the four steps of glucosylceramide biosynthetic pathway and constructed strains carrying single gene deletions.

With this study, we wanted to investigate how the enzymes putatively involved in structural modifications in the GlcCer biosynthetic pathway influence the profile of sphingoid base accumulation in *A. nidulans*. Concomitantly, we wanted to evaluate how the deletions of genes coding in the GlcCer biosynthetic pathway impair the stress response, susceptibility and growth inhibition when the strains are exposed to $[C_{10}mim]Cl$, $[P_{4\,4\,4\,12}]Cl$ or cholinium decanoate. We focused our research in the contribution of four types of enzymes, namely sphingolipid Δ4-desaturase (AN4405), Δ8-desaturase (AN4592), sphingolipid C9-methyltransferase (AN5688 and AN7375) and glucosylceramide synthase (AN8806).

To understand deeply the relevance of structural modifications in sphingoid bases, we constructed five null mutants in which the target genes in *A. nidulans* A1149 strain were replaced with *A. fumigatus pyrG* gene (*pyrG*^{Af}). As an approach to verify successful homologous recombination we resorted to differential recognition of restriction enzymes between the *pyrG*^{Af} and target gene sequences. Data presented in Figures 3.1 and 3.2 indicate that the deletion cassettes were correctly inserted at the target loci, generating ΔAN4405, ΔAN4592, ΔAN5688, ΔAN7375, ΔAN8806 strains deficient in one of the four steps of the GlcCer pathway. At the time that we were generating these null mutants, a study with the functional characterisation of AN4592, AN5688, AN7375 and AN8806 genes, named as *sdeA*, *smtA*, *smtB* and *gcsA*, respectively, was published (78). However, the suggested standard name of AN4592 (*sdeA*) is already in use for gene AN6731, which is described in the *Aspergillus* Genome Database.

A distinct accumulation profile of several sphingoid bases using a previously established HPLC method (113) could be detected in the mutant strains after 24 hours of growth, without any stress imposition (Figure 3.3). In order to simplify the discussion of these data, a summary of accumulated peaks is shown in Table 4.1. Analysis of extracted sphingoid bases from the wild-type strain indicated that the predominant sphingoid base in *A. nidulans* is phytosphingosine (PHS). In the case of the ΔAN4405 strain, the amount of dihydrosphingosine (DHS) was greatly elevated. Since DHS is the substrate of sphingolipid Δ4-desaturase enzyme, the first step of GlcCer pathway, when this enzyme is impaired an increase of DHS and the absence of its product, sphingosine (SPH), are expected. These findings are in agreement with the total sphingoid base analysis of *S. pombe* cells deficient in sphingolipid Δ4-desaturase, which generated an increase in the levels of the precursor DHS and only basal levels of SPH (110). The disruption of the AN4592 gene, involved in the second step of GlcCer biosynthetic pathway, which consists in Δ8-desaturation of SPH, led to the accumulation of C4-saturated sphingoid base, which was confirmed by comparison with the retention time of the standard compound. The observed sphingosine accumulation is in agreement with the lipid analysis of *C. albicans* cells deficient in sphingolipid Δ8-desaturase (75). Also, a more recent study showed that impairment on this sphingolipid Δ8-desaturase in *A. nidulans* resulted in accumulation of ceramides with C4-saturated sphingoid base (78). The PHS levels were similar between the two mutants and the wild-type strain. Taken together, these data suggest that the uncharacterised gene AN4405 in fact encodes an *A. nidulans* sphingolipid Δ4-desaturase.

Intriguingly, the impairment of AN5688 or AN7375 genes led to the largest PHS accumulation, most notably for the ΔAN7375 strain. It was previously reported that the double mutant for these genes is not viable, while a single deletion of these genes does not totally impair the methylation of the sphingolipid backbone. However, this was still partially hindered, since significantly higher concentrations of GlcCer with unmethylated sphingolipid backbone (4,8-sphingadienine) were observed (78). Additionally, in the same study it was observed that the AN7375 gene possibly encoded for a more functional C9-methyltransferase. Separation by reverse phase HPLC of sphingoid bases from *Pichia pastoris* showed that the PHS and 4,8-sphingadienine have the same retention time (74). This lead us to speculate that the PHS peak that we observe in our analyses most likely corresponds to these two sphingoid bases, PHS and 4,8-sphingadienine. This hypothesis is consistent with the observed increased accumulation of the peak with retention time of 7.5 min, especially for the ΔAN7375 strain.

Finally, AN8806 deletion caused a noticeable accumulation of an unidentified compound which we designated **x** (retention time 9.55 min), and a slight accumulation of the known sphingoid bases SPH and DHS. An increase of PHS levels was also observed. However, as previously mentioned, we cannot be certain that this corresponds just to PHS. A recent study showed that impairment on the gene AN8806, functionally characterised as an *A. nidulans* glucosylceramide synthase, causes the accumulation of ceramides with methylated sphingoid backbone (78). Thus, we hypothesise that the accumulated unknown compound **x** could be the methylated sphingoid base 9-methyl-4,8-sphingadienine. In the *A. nidulans* wild-type strain we also observed a slight accumulation of the unknown compound **x**. A study analysing *A. nidulans* relative abundance of the intermediates involved in GlcCer synthesis revealed high levels of GlcCer with a 9-methyl-4,8-sphingadienine backbone (78), further supporting our hypothesis that the unknown compound **x** may be the sphingoid base 9-methyl-4,8-sphingadienine.

Moreover, a slight accumulation of an unknown compound (**y**) with retention time at 11.55 min was observed for all the mutants, with exception of ΔAN4592. This compound may be a fungal response to compensate the impairment in the GlcCer biosynthetic pathway. Additionally, a noticeable accumulation of compounds that are eluted between the retention time of 3.5 and 5.2 min is observed (*e.g.* compound **α**). In plants, a great structural diversity of sphingolipids is observed (114), where sphingoid bases can contain two hydroxyl groups (DHS) with up to two double bonds in the *trans*Δ4 and *cis*/*trans*Δ8 positions or three hydroxyl groups (PHS) with a double bond in *cis*/*trans*Δ8 positions (115). Our hypothesis is that *A. nidulans* may produce structural modifications in sphingoid bases similar to those observed in plants. Nonetheless, further analyses need to be performed to understand the complexity and diversity of these structural modifications in filamentous fungi, as well as which genes and enzymes are responsible for them.

Table 4.1. Summary of data present in Figure 3.3 that demonstrated the chromatographic profile of lipid extracts from cultures after 24 hours of growth without stress imposition. ↑ Indicates level of accumulation and ─ indicates that no noticeable accumulation of compound was observed. PHS = phytosphingosine; SPH = sphingosine; DHS = dihydrosphingosine. *PHS peak may correspond to two sphingoid bases, PHS and 4,8-sphingadienine.

Strains	**Resolved peaks** (retention time in min)					
	PHS * (7.5 min)	**SPH** (10.55 min)	**DHS** (13.7 min)	**α** (3.8 min)	**x** (9.55 min)	**y** (11.55 min)
WT	↑	─	─	↑	↑	─
ΔAN4405	↑	─	↑	↑↑	─	↑
ΔAN4592	↑	↑	─	↑	─	─
ΔAN5688	↑↑↑	─	↑	↑↑	─	↑
ΔAN7375	↑↑↑↑	─	↑	↑	─	↑
ΔAN8806	↑↑	↑	↑	↑	↑↑	↑

Previous studies in our lab, using *A. nidulans* FGSC A4, showed that, after 24 hours, [C_{10}mim]Cl induces a similar accumulation pattern to that observed in this study (113), since this ionic liquid led to a large accumulation of an unknown compound, which eluted right after the PHS. In this study (summary of data is represented in Table 4.2), the observed accumulation of the unknown compound **i** in all the mutant strains suggests that this is not likely to be one of the intermediates of the GlcCer biosynthetic pathway. Still, exposure to this ionic liquid may induce different structural modifications in the sphingoid backbone, probably for the synthesis of molecules with signalling functions in this fungus. Taking into account the previous hypothesis, that the PHS peak corresponds to two sphingoid bases, PHS and 4,8-sphingadienine, the large reduction of this peak in ΔAN5688 and ΔAN7375 strains and its increase for ΔAN4405 strain suggests that this ionic liquid mainly induces a slight accumulation of PHS and not of 4,8-sphingadienine. In fact, in this stress condition we observed decreased or equal levels of all the intermediates of the GlcCer pathway, which suggests that the fungus does not respond to [C_{10}mim]Cl stress through this pathway. Since [C_{10}mim]Cl causes some level of cell wall damage (113), it is possible that the fungus is responding to this stress through the synthesis of the unknown compound **i** that might play an important role as a signalling molecule for the cell wall integrity pathway in *A. nidulans*. The function of sphingolipid intermediates as activators of this pathway in *S. cerevisiae* has already been reported (116).

Although it appears that all mutants are responding to the stress induced by [C_{10}mim]Cl through synthesis of the unknown compound **i**, its amount may be correlated with the susceptibility to this ionic liquid, since we observed that the ΔAN4405 and ΔAN4592 strains have higher susceptibility (Table 3.1) and synthesise lower amounts of compound **i**. Moreover the ΔAN5688, ΔAN7375 and ΔAN8806 strains that showed increased tolerance (Table 3.1), accumulated a greater amount of compound **i** and of compound **ii** (retention time 8.4 min) that may also be related to the fungal tolerance to this ionic liquid. However, further analyses need to be performed to identify compounds **i** and **ii** especially as to understand their roles, if any,

in the cell wall integrity pathway. Sphingolipids are present in the fungal cell membranes as structural components. Intriguingly, the growth ability of mutants in solid medium does not seem to be significantly compromised in the presence of [C_{10}mim]Cl (Figure 3.4). Our first guess was that the ionic liquid availability in the solid medium is lower, hindering its interaction with the cell wall and membranes of the fungus. However, a similar study showed that *A. nidulans* AN4592, AN5688, AN7375 and AN8806 deletions promoted resistance to the cell-wall-damaging agents congo red and calcofluor white (78). Additionally, is was observed for *C. neoformans* that the impairment of intermediates of GlcCer pathway alters membrane composition and affects fungal membrane rigidity, which indicates that specific sphingolipid structures are required for proper fungal membrane organization and integrity (76). Overall, this suggests that GlcCer synthesis impairment and, ultimately, the lack of production of its intermediates, alters the membrane fluidity, which may activate a compensatory mechanism that leads to a more rigid cell wall architecture in null mutants to retain viability. This hypothesis is consistent with the observed growth ability of null mutants in solid medium containing [C_{10}mim]Cl.

Table 4.2. Summary of data present in Figure 3.8 (A and C) that demonstrated the chromatographic profile of lipid extracts from cultures after 4 hours of stress imposition by [C_{10}mim]Cl. ↑ and ↓ indicates increase and decrease, respectively, of accumulation compared to control (without stress imposition, Figure 3.7), **=** indicates similar level of compound compared to control and ─ indicates that no noticeable accumulation was observed.
PHS = phytosphingosine; SPH = sphingosine; DHS = dihydrosphingosine. *****PHS peak may correspond to two sphingoid bases, PHS and 4,8-sphingadienine. #Compound ***x*** may correspond to the sphingoid base 9-methyl-4,8-sphingadienine.

Strains	**Resolved peaks** (retention time in min)					
	*** PHS and 4,8-sphingadienine** (7.5 min)	**SPH** (10.55 min)	**DHS** (13.7 min)	**i** (8.0 min)	**ii** (8.4 min)	**# 9-methyl-4,8-sphingadienine** (9.55 min)
WT	↑	─	─	↑	─	─
ΔAN4405	↑	─	=	↑	─	─
ΔAN4592	=	=	─	↑	─	─
ΔAN5688	↓↓	─	↓	↑↑	↑	─
ΔAN7375	↓↓↓	─	↓	↑↑↑	↑	─
ΔAN8806	=	=	↓	↑↑↑	↑	=

In earlier studies we were able to observe that [$P_{4\,4\,4\,12}$]Cl induces a differential accumulation of sphingoid bases in *A. nidulans* FGSC A4, most notably of sphingosine (SPH) which is more evident after 24 hours of exposure (117). In this study (summary of data is represented in Table 4.3), an increase of the peak initially assigned to PHS was observed, yet this more likely corresponds to an accumulation of 4,8-sphingadienine. Moreover, although not so pronounced, we also detected accumulation of the

intermediates of the GlcCer pathway SPH and 9-methyl-4,8-sphingadienine, suggestive of their involvement in the fungal response to the stress imposed by $[P_{4\,4\,4\,12}]Cl$. Other studies have shown that the increase of sphingosine-1-phosphate, which is derived from sphingosine, is associated with apoptosis suppression and regulation of signal-transduction pathways (118). Since the levels of signalling molecules in cells are tightly regulated in a spatial-temporal manner (119), this can imply that the exposure time used for this ionic liquid was insufficient to observe a significant response. Thus, further studies with different times of exposure to this ionic liquid need to be performed to assess if *A. nidulans* response involves SPH production. Measurement of the expression levels of genes involved in the phosphorylation of SPH might provide a clear answer to this unsolved aspect.

Regarding the susceptibility assays, in liquid media we observed a similar effect on both mutant and wild-type strains (Table 3.1) but, interestingly, when in solid medium all five mutants displayed an increased resistance to the $[P_{4\,4\,4\,12}]Cl$ stress (Figure 3.5). As previous studies have shown, $[P_{4\,4\,4\,12}]Cl$ is able to damage the fungal cell wall (96), but its likely lower bioavailability in solid medium might hinder its interaction with the fungal cell wall and membrane, which can be misinterpreted as an added resistance. On the other hand, as stipulated above, the lower growth inhibition in solid medium might be due to a compensatory mechanism that increases cell wall rigidity in null mutants, owing to GlcCer pathway impairment.

Table 4.3. Summary of data present in Figure 3.8 (C and D) that demonstrated the chromatographic profile of lipid extracts from cultures after 4 hours of stress imposition by $[P_{4\,4\,4\,12}]Cl$. ↑ and ↓ indicates increase and decrease, respectively, of accumulation compared to control (without stress imposition, Figure 3.7), **=** indicates similar level of compound compared to control and **—** indicates that no noticeable accumulation was observed.
PHS = hytosphingosine; SPH = sphingosine; DHS = dihydrosphingosine. *****PHS peak may correspond to two sphingoid bases, PHS and 4,8-sphingadienine. #Compound ***x*** may correspond to the sphingoid base 9-methyl-4,8-sphingadienine.

Strains	**Resolved peaks** (retention time in min)			
	*** PHS and 4,8-sphingadienine** (7.5 min)	**SPH** (10.55 min)	**DHS** (13.7 min)	**# 9-methyl-4,8-sphingadienine** (9.55 min)
WT	↑↑	—	—	—
ΔAN4405	↑↑	—	↑	—
ΔAN4592	↑↑	↑	—	—
ΔAN5688	↑	—	↑	—
ΔAN7375	↑	—	↑	—
ΔAN8806	↑↑↑	↑	↑	↑↑

The cholinium decanoate mechanism of toxicity remains unclear, however, it is known that this ionic liquid is unable to either permeabilise the plasma membrane or damage the fungal cell wall (113). It has been previously proposed that consumption of the cholinium cation led to an accumulation of the toxic compound cyanide (97), which toxicity effect is related with production of reactive oxygen species (ROS) (120). In this study (summary of data is represented in Table 4.4), we observed that after 4 hours of exposure, cholinium decanoate seems to mainly induce an increase of the PHS peak and an increase of DHS levels for ΔAN4405, ΔAN7375 and ΔAN8806. As previously mentioned we cannot be certain that the increase in the peak assigned initially to PHS corresponds solely to the presence of this sphingoid base. As ΔAN4405 and ΔAN4452 strains are unable to produce 4,8-sphingadienine, we can fairly assume that the accumulated compound corresponds mostly to PHS. In fact, in this stress condition we have not observed an increase of the intermediates of the GlcCer pathway. Accumulation of PHS and DHS have been shown to possess a fungicidal activity in *A. nidulans* through induction of apoptosis, a process that is suspected to be associated with the accumulation of reactive oxygen species (ROS) (59). As all strains apparently respond to this ionic liquid similarly, we believe that the observed sphingolipid accumulation profile, increased PHS and DHS, is not a compensatory mechanism/pathway to antagonize the imposed stress but instead a direct consequence of the ionic liquid toxic effect. Further studies to understand whether cholinium decanoate toxicity mechanism is related to the proposed hypothesis are however required.

Although all strains show a similar chromatographic profile, differences in the mutants' susceptibility were observed. In liquid media ΔAN4405, ΔAN4452 and ΔAN8806 strains revealed higher susceptibility to this ionic liquid (Table 3.1) and in solid media the last two demonstrated the highest growth inhibition (Figure 3.6). Previous studies showed that *A. nidulans* decreases cholinium decanoate concentration in the growth medium along the time (98), and can uptake the cholinium cation (121). Most likely cholinium decanoate might be uptaken and biodegraded by this fungus. Since impairment of the GlcCer pathway intermediates leads to a disrupted membrane organisation, higher rigidity and altered transmembrane transporters organisation (76), this can translate into a decreased ability to balance the internalised amounts of the cholinium decanoate, increasing its toxic effect. This hypothesis is consistent with the observed increased susceptibility of ΔAN4405, ΔAN4452 and ΔAN8806 strains in the presence of cholinium decanoate. However, further studies need to be performed in order to unravel the mechanism of action of this ionic liquid.

Table 4.4. Summary of data present in Figure 3.9 (A and B) that demonstrated the chromatographic profile of lipid extracts from cultures after 4 hours of stress imposition by cholinium decanoate. ↑ and ↓ indicates increase and decrease, respectively, of accumulation compared to control (without stress imposition, Figure 3.7), = indicates similar level of compound compared to control and ─ indicates that no noticeable accumulation was observed.
PHS = phytosphingosine; SPH = sphingosine; DHS = dihydrosphingosine. *PHS peak may correspond to two sphingoid bases, PHS and 4,8-sphingadienine. #Compound ***x*** may correspond to the sphingoid base 9-methyl-4,8-sphingadienine.

Strains	**Resolved peaks** (retention time in min)			
	*** PHS and 4,8-sphingadienine** (7.5 min)	**SPH** (10.55 min)	**DHS** (13.7 min)	**# 9-methyl-4,8-sphingadienine** (9.55 min)
WT	↑↑	─	─	─
ΔAN4405	↑↑	─	↑↑	─
ΔAN4592	↑↑	=	─	─
ΔAN5688	↑↑	─	↓	─
ΔAN7375	↑↑	─	↑↑	─
ΔAN8806	↑↑	=	↑↑	=

Following the observed effects of ionic liquid stress, we aimed to understand how the deletion of each element of the sphingolipid biosynthesis could influence the fungal response to antifungal drugs. For this we tested the susceptibility of the mutant strains to a selected set of known antifungal drugs: itraconazole, fluconazole, amphotericin B, flucytosine and terbinafine. Our results indicate that the mutant strains in the GlcCer pathway present very distinct profiles of susceptibility or resistance to different antifungal drugs, and the summary of data is represented in Table 4.5. Although this constitutes a preliminary study of the impact of GlcCer pathway on the action of antifungal drugs, these observations are promising and warrant further investigation.

The susceptibility analysis of ΔAN5688 and ΔAN7375 strains reveals that they display increased resistance to fluconazole, itraconazole and terbinafine. These data are very interesting, since the single deletion of either of these two genes does not totally impair the GlcCer pathway, although it led to different pattern of accumulation of sphingoid bases, mostly of 4,8-sphingadienine (Figure 3.3D and E, Table 4.1). As fluconazole, itraconazole and terbinafine have a similar mechanism of action, inhibition of the ergosterol biosynthetic pathway (even though in different steps) (122,123), this is highly suggestive that increased levels of 4,8-sphingadienine could be related to resistance to these antifungal drugs. Further analysis of the response of ΔAN5688 and ΔAN7375 strains in presence of these drugs, including the chromatographic analysis of sphingoid bases profile, need to be performed in order to understand whether 4,8-sphingadienine is in fact involved in the mechanism of resistance to these antifungal drugs.

We also observed an increased resistance of ΔAN4405 and ΔAN8806 strains to amphotericin B, while the remaining mutants showed a similar response to this antifungal drug. The mechanism of action of

amphotericin B is based on the effect of both ergosterol binding and pore formation; the sterol binding is necessary for its antifungal activity since the channel formation is dependent of ergosterol binding (124). It was demonstrated that *A. nidulans* deficient in AN8806 gene (glucosylceramide synthase) exhibits a significant reduction of triacylglycerol and sterol content (78). Since this mutant displays membranes containing lower amounts of ergosterol, the antifungal drug would have less interaction sites which is translated in increased resistance. Although there is no study in which triacylglycerol and sterol abundance were analysed in the ΔAN4405 strain, our results suggest that impairment of sphingolipid Δ4-desaturase (first step of GlcCer pathway) may also lead to reduction of ergosterol levels. Moreover, the analysis of this neutral lipid abundance in the ΔAN4592, ΔAN5688 or ΔAN7374 strains showed similar levels of these lipids to those in wild-type strain (78), which could explain why no alterations were observed in their susceptibility to amphotericin B.

Moreover, we observed that all the mutant strains are more susceptible to action of flucytosine (despite not statistically significant, the ΔAN7375 also showed lower EC_{50} value). It was shown that ceramides are important for cell cycle progression and their unbalancing may lead to alterations in the cell cycle (107). Since flucytosine, a pyrimidine analogue, is an S-phase-specific drug that interferes with DNA and RNA synthesis (53,125), we believe that the unbalancing of ceramide levels that may occur in our GlcCer pathway mutants could alter the cell cycle progression and, consequently, affect their susceptibility to this antifungal drug. Still, further studies need to be performed to validate this hypothesis.

Table 4.5. Summary of data present in Figure 3.10 that demonstrated the EC_{50} (drug concentration producing 50 % of the effect). ↑ and ↓ indicates increase and decrease, respectively, of the EC_{50} values compared to wild-type strain, **=** indicates similar EC_{50} values compared to wild-type.

Strains	**Susceptibility to antifungal drugs** (mechanism of action)				
	Itraconazole (Inhibition of ergosterol biosynthesis)	**Fluconazole** (Inhibition of ergosterol biosynthesis)	**Amphotericin B** (Disruption of cell membrane through binding to ergosterol)	**Terbinafine** (Inhibition of ergosterol biosynthesis)	**Flucytosine** (Inhibition of fungal RNA and DNA synthesis)
ΔAN4405	=	↓	↑	↑	↓
ΔAN4592	=	↓	=	↑	↓
ΔAN5688	↑	↑	=	↑	↓
ΔAN7375	↑	↑	=	↑	=
ΔAN8806	=	↓	↑	=	↓

Overall, this study showed that sphingolipid intermediates and their role in the fungal stress response deserve further investigation as they can be a promising target for future antifungal drug development. In this context, future studies should attempt to answer some key questions raised throughout the discussion section of the thesis, namely to confirm the peak assignment of the hypothesised mixture of two sphingoid bases, PHS and 4,8-sphingadienine. The use of the standard compound of 4,8-sphingadienine, which is now commercially available, will show whether this compound elutes chromatographically with the same retention time as PHS; if this is verified (as highly expected), the established HPLC method will be modified to be able to resolve PHS and 4,8-sphingadienine. Separation of these two sphingoid bases will enable us to determine the accumulation levels of each compound after exposure to ionic liquids and to better understand the fungal response to the imposed stress. To characterise the unknown sphingoid bases we can rely on the use of GC-MS, this knowledge will help to better understand the complexity and diversity of the structural modifications that sphingoid bases can undergo in *A. nidulans*. Additionally, to better understand whether the impairment of the GlcCer pathway triggers a compensatory mechanism that leads to increased cell wall rigidity, the expression levels of genes coding for elements of the cell wall integrity pathway and for enzymes directly involved in cell wall biosynthesis, need to be assessed by quantitative real-time PCR assays. Unknown genes and/or pathways can then be identified relying on whole transcriptomic profiling tools as RNAseq.

To further analyse the response of the GlcCer pathway mutants in the presence of antifungal drugs we will rely on the same methods used in this study, namely chromatographic analysis of sphingoid bases profile and fungal radial growth in solid medium. Additionally, it would be interesting to add to these tests an antifungal drug with action in the cell wall, such as caspofungin.

CHAPTER 5 – Conclusion

The work developed in this thesis aimed to unravel how sphingolipid biosynthesis impacts stress responses in *Aspergillus nidulans*. The working strategy was defined by the previous hypothesis that sphingolipid intermediates act as secondary messengers in response to the stress imposed by ionic liquids.

The overall working strategy included the identification of putative genes encoding enzymes involved in structural modifications of sphingoid bases from the glucosylceramide (GlcCer) pathway in *A. nidulans* and the construction of single deletion strains for the identified genes. *Aspergillus nidulans* mutants were grown in presence or not of the ionic liquids [C_{10}mim]Cl, cholinium decanoate or [$P_{4\,4\,4\,12}$]Cl to analyse the differential accumulation of sphingoid bases. To complement these analyses, for each deleted strain, the minimal inhibitory concentrations (MIC) for each ionic liquid were determined as well as their impact on fungal radial growth on solid minimal medium. Additionally, a preliminary test was performed where the susceptibility of the deleted strains to the known antifungal drugs itraconazole, fluconazole, amphotericin B, flucytosine and terbinafine was assessed.

The characterisation of glucosylceramide pathway mutants through liquid chromatography analyses exposed the accumulation profile of each strain and allowed correlation of the observed differential compounds to sphingolipid intermediates of this pathway. Moreover, it was possible to verify that the uncharacterised gene AN4405 encodes an *A. nidulans* sphingolipid Δ4-desaturase. The major drawback of our strategy was the lack of confirmation that the two sphingoid bases, phytosphingosine (PHS) and 4,8-sphingadienine, eluted at the same retention time. This was likely due to the HPLC method used which requires further optimisation. The mutant response to [C_{10}mim]Cl stress allowed us to conclude that the fungus does not respond to this stress through the GlcCer biosynthetic pathway. However, exposure to this ionic liquid led to an increased accumulation of unknown sphingoid bases that might play an important role as signalling molecules in *A. nidulans*. Mutant exposure to the other two ionic liquids, [$P_{4\,4\,4\,12}$]Cl and cholinium decanoate, does not allow us to clearly understand how the fungus responds to these stresses. Still, the sphingoid bases sphingosine and 9-methyl-4,8-sphingadienine might be involved in fungal response to [$P_{4\,4\,4\,12}$]Cl. The susceptibility analysis of mutant strains of GlcCer pathway to a selected set of known antifungals indicated that these mutants present very distinct susceptibility or resistance profiles to different antifungal drugs. Although this constitutes a preliminary study, our observations are promising and merit further investigation.

The emergence of novel fungal pathogens, the growth of the population at risk and the lack of novel antifungal drugs, clearly justify the efforts done in the present thesis. Our aim is not to propose a new drug but to fill important gaps in fungal biology, particularly on the strategies that fungi use to circumvent the stress imposed by chemicals. The data herein presented further reinforce the significance of the sphingolipid pathway in stress responses, strengthening our interest in exploiting ionic liquids as means to unravel

complex biosynthetic pathways in filamentous fungi. We wish to deliver important insights, which in future may support the improvement of established drugs. More importantly, our study may lead to the discovery of new fungal targets and the design of novel drugs.

REFERENCES

1. Deacon, J. W. (2006) Introduction: the fungi and fungal activities. in *Fungal Biology*, Fourth Ed., Blackwell Publishing. pp 1-15
2. Murray, P. R., Rosenthal, K. S., and Pfaller, M. A. (2015) Fungal Classification, Structure, and Replication. in *Medical microbiology*, Eighth Ed., Elsevier. pp 568-574
3. Money, N. P. (2016) What is a fungus? in *Fungi: A Very Short Introduction*, Oxford University Press. pp 1-17
4. Webster, J., and Weber, R. (2007) Introduction to fungi. Third Ed., Cambridge University Press. pp 1-32
5. Boyce, K. J., and Andrianopoulos, A. (2006) Morphogenesis: control of cell types and shape. in *The Mycota I - Growth, differentiation and sexuality* (Kües, U., and Fischer, R. eds.), Second Ed., Springer. pp 3-5
6. Carlile, M. J., Watkinson, S. C., and Gooday, G. W. (2001) Fungal cells and vegetative growth. in *The Fungi*, Second Ed., Elsevier Academic Press. pp 85-87
7. Carlile, M. J., Watkinson, S. C., and Gooday, G. W. (2001) Spores, Dormancy and Dispersal. in *The fungi*, Second Ed., Elsevier Academic Press. pp 186-194
8. Fischer, R., and Kües, U. (2006) Asexual sporulation in mycelial fungi. in *The Mycota I - Growth, Differentiation and Sexuality* (Kües, U., and Fischer, R. eds.), Second Ed., Springer. pp 263-292
9. Zickler, D. (2006) Meiosis in Mycelial Fungi. in *The Mycota I - Growth, differentiation and sexuality* (Kües, U., and Fischer, R. eds.), Second Ed., Springer. pp 415-421
10. Deacon, J. W. (2006) Fungal ecology: saprotrophs. in *Fungal Biology*, Fourth Ed., Blackwell Publishing. pp 213-215
11. Paszkowski, U. (2006) Mutualism and parasitism: the yin and yang of plant symbioses. *Curr. Opin. Plant Biol.* **9**, 364-370
12. Kalač, P. (2016) Edible Mushrooms: Chemical Composition and Nutritional Value. Elsevier. pp 1-6
13. Murphy, R. A., and Horgan, K. A. (2005) Antibiotics, Enzymes and Chemical Commodities from Fungi. in *Fungi: biology and applications* (Kavanagh, K. ed.), First Ed., Wiley. pp 113-143
14. Goicoechea, N., and Antolín, M. C. (2017) Increased nutritional value in food crops. *Microbial Biotechnology* **0**, 1-4
15. Gill, S. S., Gill, R., Trivedi, D. K., Anjum, N. A., Sharma, K. K., Ansari, M. W., Ansari, A. A., Johri, A. K., Prasad, R., and Pereira, E. (2016) *Piriformospora indica*: potential and significance in plant stress tolerance. *Frontiers in microbiology* **7**
16. Fisher, M. C., Henk, D. A., Briggs, C. J., Brownstein, J. S., Madoff, L. C., McCraw, S. L., and Gurr, S. J. (2012) Emerging fungal threats to animal, plant and ecosystem health. *Nature* **484**
17. Carlile, M. J., Watkinson, S. C., and Gooday, G. W. (2001) Genetic Variation and Evolution. in *The Fungi*, Second Ed., Elsevier Academic Press. pp 245-263
18. Whiteway, M., and Bachewich, C. (2005) Fungal Genetics. in *Fungi: biology and applications* (Kavanagh, K. ed.), First Ed., Wiley. pp 35-62
19. Cavalier-Smith, T., and Chao, E. (1995) The opalozoan Apusomonas is related to the common ancestor of animals, fungi, and choanoflagellates. *Proceedings of the Royal Society of London B: Biological Sciences* **261**, 1-6
20. Whittaker, R. H. (1969) New concepts of kingdoms of organisms. *Science* **163**, 150-160
21. Cavalier-Smith, T. (1998) A revised six-kingdom system of life. *Biological Reviews* **73**, 203-266
22. Cavalier-Smith, T. (2004) Only six kingdoms of life. *Proceedings of the Royal Society B: Biological Sciences* **271**, 1251
23. Hibbett, D. S., Binder, M., Bischoff, J. F., Blackwell, M., Cannon, P. F., Eriksson, O. E., Huhndorf, S., James, T., Kirk, P. M., and Lücking, R. (2007) A higher-level phylogenetic classification of the Fungi. *Mycol. Res.* **111**, 509-547
24. Martin Carr, and Baldauf, S. L. (2011) The Protistan Origins of Animals and Fungi. in *The Mycota XIV - Evolution of fungi and fungal-like organisms* (Pöggeler, S., and Wöstemeyer, J. eds.), Springer. pp 3-18
25. Schoch, C. L., Sung, G.-H., López-Giráldez, F., Townsend, J. P., Miadlikowska, J., Hofstetter, V., Robbertse, B., Matheny, P. B., Kauff, F., and Wang, Z. (2009) The *Ascomycota* tree of life: a phylum-wide phylogeny clarifies the origin and evolution of fundamental reproductive and ecological traits. *Syst. Biol.* **58**, 224-239

26. Moore, D., Robson, G. D., and Trinci, A. P. (2011) Natural classification of fungi. in *21st century guidebook to fungi*, First Ed., Cambridge University Press. pp 41-79

27. Money, N. (2015) Fungal Diversity. in *The Fungi* (Watkinson, S. C., Boddy, L., and Money, N. eds.), Third Ed., Elsevier. pp 1-37

28. Gabaldón, T., Naranjo-Ortíz, M. A., and Marcet-Houben, M. (2016) Evolutionary genomics of yeast pathogens in the *Saccharomycotina*. *FEMS Yeast Res.* **16**, 1-10

29. James, T. Y., Kauff, F., Schoch, C. L., Matheny, P. B., Hofstetter, V., Cox, C. J., Celio, G., Gueidan, C., Fraker, E., and Miadlikowska, J. (2006) Reconstructing the early evolution of Fungi using a six-gene phylogeny. *Nature* **443**, 818-822

30. Hawksworth, D. L. (1991) The fungal dimension of biodiversity: magnitude, significance, and conservation. *Mycol. Res.* **95**, 641-655

31. Hawksworth, D., and Lücking, R. (2017) Fungal Diversity Revisited: 2.2 to 3.8 Million Species. *Microbiology spectrum* **5**

32. Gallegos, F. A. C., Hernandez, V. F., Michel, M. M., Victoriano, L. F., and Herrera, R. R. (2016) Molecular Evolution of *Aspergillus*. in *New and Future Developments in Microbial Biotechnology and Bioengineering: Aspergillus System Properties and Applications* (Gupta, V. K. ed.), Elsevier. pp 41-45

33. Baker, S. E., and Bennett, J. W. (2007) An Overview of the Genus Aspergillus. in *The Aspergilli: genomics, medical aspects, biotechnology, and research methods* (Goldman, G. H., and Osmani, S. A. eds.), CRC press. pp 3-11

34. Park, H.-S., Jun, S.-C., Han, K.-H., Hong, S.-B., and Yu, J.-H. (2017) Diversity, Application, and Synthetic Biology of Industrially Important Aspergillus Fungi. *Adv. Appl. Microbiol.* **100**, 161-202

35. Galagan, J. E., Calvo, S. E., Cuomo, C., Ma, L.-J., Wortman, J. R., Batzoglou, S., Lee, S.-I., Baştürkmen, M., Spevak, C. C., and Clutterbuck, J. (2005) Sequencing of *Aspergillus nidulans* and comparative analysis with *A. fumigatus* and *A. oryzae*. *Nature* **438**, 1105-1115

36. Gavrias, V., Timberlake, W. E., and Adams, T. H. (2001) *Aspergillus nidulans*. in *Encyclopedia of Genetics* (Brenner, S., and Miller, J. H. eds.), Academic Press. pp 106-111

37. Davis, R. H. (2003) The microbial models of molecular biology: from genes to genomes. Oxford University Press. pp 47-60

38. Casselton, L., and Zolan, M. (2002) The art and design of genetic screens: filamentous fungi. *Nat. Rev. Genet.* **3**, 683

39. Braus, G. H., Krappmann, S., and Eckert, S. E. (2002) Sexual development in ascomycetes: fruit body formation of *Aspergillus nidulans*. in *Molecular Biology of Fungal Development* (Osiewacz, H. D. ed.), Marcel Dekker. pp 215-244

40. Richardson, M. D., and Warnock, D. W. (2012) Fungi as human pathogens. in *Fungal infection: diagnosis and management*, Fourth Ed., John Wiley & Sons. pp 5-11

41. Brown, G. D., Denning, D. W., Gow, N. A., Levitz, S. M., Netea, M. G., and White, T. C. (2012) Hidden killers: human fungal infections. *Sci. Transl. Med.* **4**, 165rv113-165rv113

42. Slavin, M., Van Hal, S., Sorrell, T., Lee, A., Marriott, D., Daveson, K., Kennedy, K., Hajkowicz, K., Halliday, C., and Athan, E. (2015) Invasive infections due to filamentous fungi other than *Aspergillus*: epidemiology and determinants of mortality. *Clin. Microbiol. Infect.* **21**, 490. e491-490. e410

43. Araujo, R., Pina-Vaz, C., and Rodrigues, A. G. (2010) Mould Infections: A Global Threat to Immunocompromised Patients. in *Combating fungal infections: problems and remedy* (Ahmad, I., Owais, M., Shahid, M., and Aqil, F. eds.), Springer pp 1-21

44. Roemer, T., and Krysan, D. J. (2014) Antifungal drug development: challenges, unmet clinical needs, and new approaches. *Cold Spring Harbor perspectives in medicine* **4**, a019703

45. Lewis, R. E., and Fothergill, A. W. (2015) Antifungal Agents. in *Diagnosis and Treatment of Fungal Infections* (Hospenthal, D. R., and Rinaldi, M. G. eds.), Second Ed., Springer. pp

46. Campoy, S., and Adrio, J. L. (2017) Antifungals. *Biochem. Pharmacol.* **133**, 86-96

47. Kakeya, H., Miyazaki, Y., Senda, H., Kobayashi, T., Seki, M., Izumikawa, K., Yanagihara, K., Yamamoto, Y., Tashiro, T., and Kohno, S. (2008) Efficacy of SPK-843, a novel polyene antifungal, in comparison with amphotericin B, liposomal amphotericin B, and micafungin against murine pulmonary aspergillosis. *Antimicrob. Agents Chemother.* **52**, 1868-1870

48. Hamill, R. J. (2013) Amphotericin B formulations: a comparative review of efficacy and toxicity. *Drugs* **73**, 919-934

49. Saag, M. S., and Dismukes, W. E. (1988) Azole antifungal agents: emphasis on new triazoles. *Antimicrob. Agents Chemother.* **32**, 1-8

50. Maertens, J. (2004) History of the development of azole derivatives. *Clin. Microbiol. Infect.* **10**, 1-10

51. Peyton, L., Gallagher, S., and Hashemzadeh, M. (2015) Triazole antifungals: a review. *Drugs Today (Barc)* **51**, 705-718

52. Aronson, J. K. (2015) Meyler's side effects of drugs: the international encyclopedia of adverse drug reactions and interactions. Sixteenth Ed., Elsevier. pp 6-14

53. Vermes, A., Guchelaar, H.-J., and Dankert, J. (2000) Flucytosine: a review of its pharmacology, clinical indications, pharmacokinetics, toxicity and drug interactions. *J. Antimicrob. Chemother.* **46**, 171-179

54. Kathiravan, M. K., Salake, A. B., Chothe, A. S., Dudhe, P. B., Watode, R. P., Mukta, M. S., and Gadhwe, S. (2012) The biology and chemistry of antifungal agents: a review. *Bioorg. Med. Chem.* **20**, 5678-5698

55. Perfect, J. R. (2017) The antifungal pipeline: a reality check. *Nat. Rev. Drug Discovery*

56. Arendrup, M. C., and Perlin, D. S. (2014) Echinocandin resistance: an emerging clinical problem? *Curr. Opin. Infect. Dis.* **27**, 484

57. Rollin-Pinheiro, R., Singh, A., Barreto-Bergter, E., and Del Poeta, M. (2016) Sphingolipids as targets for treatment of fungal infections. *Future medicinal chemistry* **8**, 1469-1484

58. Jenkins, G. M., Richards, A., Wahl, T., Mao, C., Obeid, L., and Hannun, Y. (1997) Involvement of yeast sphingolipids in the heat stress response of *Saccharomyces cerevisiae*. *J. Biol. Chem.* **272**, 32566-32572

59. Cheng, J., Park, T.-S., Chio, L.-C., Fischl, A. S., and Xiang, S. Y. (2003) Induction of apoptosis by sphingoid long-chain bases in *Aspergillus nidulans*. *Mol. Cell. Biol.* **23**, 163-177

60. Hannun, Y. A., and Obeid, L. M. (2008) Principles of bioactive lipid signalling: lessons from sphingolipids. *Nat. Rev. Mol. Cell Biol.* **9**, 139-150

61. Zhong, W., Jeffries, M. W., and Georgopapadakou, N. H. (2000) Inhibition of Inositol Phosphorylceramide Synthase by Aureobasidin A in *Candida* and *Aspergillus* Species. *Antimicrob. Agents Chemother.* **44**, 651-653

62. Levery, S. B., Momany, M., Lindsey, R., Toledo, M. S., Shayman, J. A., Fuller, M., Brooks, K., Doong, R. L., Straus, A. H., and Takahashi, H. K. (2002) Disruption of the glucosylceramide biosynthetic pathway in *Aspergillus nidulans* and *Aspergillus fumigatus* by inhibitors of UDP-Glc: ceramide glucosyltransferase strongly affects spore germination, cell cycle, and hyphal growth. *FEBS Lett.* **525**, 59-64

63. Singh, A., and Del Poeta, M. (2016) Sphingolipidomics: An Important Mechanistic Tool for Studying Fungal Pathogens. *Frontiers in microbiology* **7**

64. Olsen, I., and Jantzen, E. (2001) Sphingolipids in bacteria and fungi. *Anaerobe* **7**, 103-112

65. Martínez-Montañés, F., and Schneiter, R. (2016) Tools for the analysis of metabolic flux through the sphingolipid pathway. *Biochimie* **130**, 76-80

66. Dickson, R. C., and Lester, R. L. (2002) Sphingolipid functions in *Saccharomyces cerevisiae*. *Biochim. Biophys. Acta* **1583**, 13-25

67. Merrill, A. H. (2002) De novo sphingolipid biosynthesis: a necessary, but dangerous, pathway. *J. Biol. Chem.* **277**, 25843-25846

68. Haak, D., Gable, K., Beeler, T., and Dunn, T. (1997) Hydroxylation of *Saccharomyces cerevisiae* ceramides requires Sur2p and Scs7p. *J. Biol. Chem.* **272**, 29704-29710

69. Nagiec, M. M., Baltisberger, J. A., Wells, G. B., Lester, R. L., and Dickson, R. C. (1994) The LCB2 gene of *Saccharomyces* and the related LCB1 gene encode subunits of serine palmitoyltransferase, the initial enzyme in sphingolipid synthesis. *Proceedings of the National Academy of Sciences* **91**, 7899-7902

70. Nagiec, M. M., Nagiec, E. E., Baltisberger, J. A., Wells, G. B., Lester, R. L., and Dickson, R. C. (1997) Sphingolipid synthesis as a target for antifungal drugs complementation of the inositol phosphorylceramide synthase defect in a mutant strain of *Saccharomyces cerevisiae* by the AUR1 gene. *J. Biol. Chem.* **272**, 9809-9817

71. Dickson, R. C., Nagiec, E. E., Wells, G. B., Nagiec, M. M., and Lester, R. L. (1997) Synthesis of mannose-(inositol-P) 2-ceramide, the major sphingolipid in *Saccharomyces cerevisiae*, requires the IPT1 (YDR072c) gene. *J. Biol. Chem.* **272**, 29620-29625

72. Ternes, P., Sperling, P., Albrecht, S., Franke, S., Cregg, J. M., Warnecke, D., and Heinz, E. (2006) Identification of fungal sphingolipid C9-methyltransferases by phylogenetic profiling. *J. Biol. Chem.* **281**, 5582-5592

73. Ternes, P., Franke, S., Zähringer, U., Sperling, P., and Heinz, E. (2002) Identification and characterization of a sphingolipid Δ4-desaturase family. *J. Biol. Chem.* **277**, 25512-25518

74. Ternes, P., Wobbe, T., Schwarz, M., Albrecht, S., Feussner, K., Riezman, I., Cregg, J. M., Heinz, E., Riezman, H., and Feussner, I. (2011) Two pathways of sphingolipid biosynthesis are separated in the yeast *Pichia pastoris*. *J. Biol. Chem.* **286**, 11401-11414

75. Oura, T., and Kajiwara, S. (2008) Disruption of the sphingolipid Δ8-desaturase gene causes a delay in morphological changes in *Candida albicans*. *Microbiology* **154**, 3795-3803

76. Singh, A., Wang, H., Silva, L. C., Na, C., Prieto, M., Futerman, A. H., Luberto, C., and Del Poeta, M. (2012) Methylation of glycosylated sphingolipid modulates membrane lipid topography and pathogenicity of *Cryptococcus neoformans*. *Cell. Microbiol.* **14**, 500-516

77. Ramamoorthy, V., Cahoon, E. B., Thokala, M., Kaur, J., Li, J., and Shah, D. M. (2009) Sphingolipid C-9 methyltransferases are important for growth and virulence but not for sensitivity to antifungal plant defensins in *Fusarium graminearum*. *Eukaryot. Cell* **8**, 217-229

78. Fernandes, C., de Castro, P., Singh, A., Fonseca, F., Pereira, M., Vila, T., Atella, G., Rozental, S., Savoldi, M., and Del Poeta, M. (2016) Functional characterization of the *Aspergillus nidulans* glucosylceramide pathway reveals that LCB Δ8-desaturation and C9-methylation are relevant to filamentous growth, lipid raft localization and Psd1 defensin activity. *Mol. Microbiol.* **102**, 488-505

79. Hartmann, D. O., and Pereira, C. S. (2016) Toxicity of Ionic Liquids: Past, Present, and Future. in *Ionic Liquids in Lipid Processing and Analysis: Opportunities and Challenges* (Xu, X., Guo, Z., and Cheong, L.-Z. eds.), First Ed., Elsevier. pp 403-421

80. Zhang, S., Lu, X., Zhou, Q., Li, X., Zhang, X., and Li, S. (2009) Ionic liquids: physicochemical properties. First Ed., Elsevier. pp 3-21

81. Petkovic, M., Seddon, K. R., Rebelo, L. P. N., and Pereira, C. S. (2011) Ionic liquids: a pathway to environmental acceptability. *Chem. Soc. Rev.* **40**, 1383-1403

82. Plechkova, N. V., and Seddon, K. R. (2007) Ionic liquids: “designer” solvents for green chemistry. in *Methods and Reagents for Green Chemistry* (Tundo, P., Perosa, A., and Zecchini, F. eds.), John Wiley & Sons. pp 105-130

83. Smiglak, M., Pringle, J., Lu, X., Han, L., Zhang, S., Gao, H., MacFarlane, D., and Rogers, R. (2014) Ionic liquids for energy, materials, and medicine. *Chem. Commun.* **50**, 9228-9250

84. Shadpour, M., and Mohammad, D. (2012) Ionic Liquids as Green Solvents: Progress and Prospects. in *Green solvents II: properties and applications of ionic liquids* (Mohammad, A., and Inamuddin eds.), Springer pp 1-33

85. Pernak, J., Rogoża, J., and Mirska, I. (2001) Synthesis and antimicrobial activities of new pyridinium and benzimidazolium chlorides. *Eur. J. Med. Chem.* **36**, 313-320

86. Bernot, R. J., Brueseke, M. A., Evans-White, M. A., and Lamberti, G. A. (2005) Acute and chronic toxicity of imidazolium-based ionic liquids on *Daphnia magna*. *Environ. Toxicol. Chem.* **24**, 87-92

87. Latała, A., Nędzi, M., and Stepnowski, P. (2009) Toxicity of imidazolium and pyridinium based ionic liquids towards algae. *Chlorella vulgaris*, *Oocystis submarina* (green algae) and *Cyclotella meneghiniana*, *Skeletonema marinoi* (diatoms). *Green Chem.* **11**, 580-588

88. Ranke, J., Mölter, K., Stock, F., Bottin-Weber, U., Poczobutt, J., Hoffmann, J., Ondruschka, B., Filser, J., and Jastorff, B. (2004) Biological effects of imidazolium ionic liquids with varying chain lengths in acute Vibrio fischeri and WST-1 cell viability assays. *Ecotoxicol. Environ. Saf.* **58**, 396-404

89. Stepnowski, P., Skladanowski, A., Ludwiczak, A., and Laczyńska, E. (2004) Evaluating the cytotoxicity of ionic liquids using human cell line HeLa. *Hum. Exp. Toxicol.* **23**, 513-517

90. Ranke, J., Müller, A., Bottin-Weber, U., Stock, F., Stolte, S., Arning, J., Störmann, R., and Jastorff, B. (2007) Lipophilicity parameters for ionic liquid cations and their correlation to in vitro cytotoxicity. *Ecotoxicol. Environ. Saf.* **67**, 430-438

91. Pernak, J., Syguda, A., Mirska, I., Pernak, A., Nawrot, J., Prądzyńska, A., Griffin, S. T., and Rogers, R. D. (2007) Choline-Derivative-Based Ionic Liquids. *Chemistry-A European Journal* **13**, 6817-6827

92. Petkovic, M., Ferguson, J. L., Gunaratne, H. N., Ferreira, R., Leitao, M. C., Seddon, K. R., Rebelo, L. P. N., and Pereira, C. S. (2010) Novel biocompatible cholinium-based ionic liquids - toxicity and biodegradability. *Green Chem.* **12**, 643-649

93. Klein, R., Müller, E., Kraus, B., Brunner, G., Estrine, B., Touraud, D., Heilmann, J., Kellermeier, M., and Kunz, W. (2013) Biodegradability and cytotoxicity of choline soaps on human cell lines: effects of chain length and the cation. *RSC Advances* **3**, 23347-23354

94. Ventura, S. P., Marques, C. S., Rosatella, A. A., Afonso, C. A., Gonçalves, F., and Coutinho, J. A. (2012) Toxicity assessment of various ionic liquid families towards *Vibrio fischeri* marine bacteria. *Ecotoxicol. Environ. Saf.* **76**, 162-168

95. Atefi, F., Garcia, M. T., Singer, R. D., and Scammells, P. J. (2009) Phosphonium ionic liquids: design, synthesis and evaluation of biodegradability. *Green Chem.* **11**, 1595-1604

96. Hartmann, D. O., and Pereira, C. S. (2013) A molecular analysis of the toxicity of alkyltributylphosphonium chlorides in *Aspergillus nidulans*. *New J. Chem.* **37**, 1569-1577

97. Martins, I., Hartmann, D. O., Alves, P. C., Planchon, S., Renaut, J., Leitão, M. C., Rebelo, L. P., and Pereira, C. S. (2013) Proteomic alterations induced by ionic liquids in *Aspergillus nidulans* and *Neurospora crassa*. *Journal of proteomics* **94**, 262-278

98. Hartmann, D. O., Shimizu, K., Siopa, F., Leitão, M. C., Afonso, C. A., Lopes, J. N. C., and Pereira, C. S. (2015) Plasma membrane permeabilisation by ionic liquids: a matter of charge. *Green Chem.* **17**, 4587-4598

99. Alves, P. C., Hartmann, D. O., Núñez, O., Martins, I., Gomes, T. L., Garcia, H., Galceran, M. T., Hampson, R., Becker, J. D., and Pereira, C. S. (2016) Transcriptomic and metabolomic profiling of ionic liquid stimuli unveils enhanced secondary metabolism in *Aspergillus nidulans*. *BMC Genomics* **17**, 284

100. Adamová, G., Gardas, R. L., Nieuwenhuyzen, M., Puga, A. V., Rebelo, L. P. N., Robertson, A. J., and Seddon, K. R. (2012) Alkyltributylphosphonium chloride ionic liquids: synthesis, physicochemical properties and crystal structure. *Dalton Trans.* **41**, 8316-8332

101. Petkovic, M., Ferguson, J. L., Gunaratne, H. N., Ferreira, R., Leitao, M. C., Seddon, K. R., Rebelo, L. P. N., and Pereira, C. S. (2010) Novel biocompatible cholinium-based ionic liquids—toxicity and biodegradability. *Green Chem.* **12**, 643-649

102. Nayak, T., Szewczyk, E., Oakley, C. E., Osmani, A., Ukil, L., Murray, S. L., Hynes, M. J., Osmani, S. A., and Oakley, B. R. (2006) A versatile and efficient gene-targeting system for *Aspergillus nidulans*. *Genetics* **172**, 1557-1566

103. Szewczyk, E., Nayak, T., Oakley, C. E., Edgerton, H., Xiong, Y., Taheri-Talesh, N., Osmani, S. A., and Oakley, B. R. (2006) Fusion PCR and gene targeting in *Aspergillus nidulans*. *Nat. Protoc.* **1**, 3111-3120

104. Yelton, M. M., Hamer, J. E., and Timberlake, W. E. (1984) Transformation of *Aspergillus nidulans* by using a trpC plasmid. *Proceedings of the National Academy of Sciences* **81**, 1470-1474

105. Osmani, A. H., Oakley, B. R., and Osmani, S. A. (2006) Identification and analysis of essential *Aspergillus nidulans* genes using the heterokaryon rescue technique. *Nat. Protoc.* **1**, 2517-2526

106. Innis, M. A., and Gelfand, D. (2012) Optimization of PCRs. in *PCR Protocols: A Guide to Methods and Applications*, Academic Press: San Diego, CA, USA. pp 3-12

107. Cheng, J., Park, T.-S., Fischl, A. S., and Xiang, S. Y. (2001) Cell cycle progression and cell polarity require sphingolipid biosynthesis in *Aspergillus nidulans*. *Mol. Cell. Biol.* **21**, 6198-6209

108. Yoon, H.-T., Yoo, H.-S., Shin, B.-K., Lee, W.-J., Kim, H.-M., Hong, S.-P., Moon, D.-C., and Lee, Y.-M. (1999) Improved fluorescent determination method of cellular sphingoid bases in high-performance liquid chromatography. *Arch. Pharmacal Res.* **22**, 294-299

109. NCCLS. (2002) *Reference Method for Broth Dilution Antifungal Susceptibility Testing of Yeasts*, Second ed., National committee for clinical laboratory standards document M27-A2, Wayne, Pennsylvania

110. Garton, S., Michaelson, L. V., Beaudoin, F., Beale, M. H., and Napier, J. A. (2003) The dihydroceramide desaturase is not essential for cell viability in *Schizosaccharomyces pombe*. *FEBS Lett.* **538**, 192-196

111. Oura, T., and Kajiwara, S. (2010) *Candida albicans* sphingolipid C9-methyltransferase is involved in hyphal elongation. *Microbiology* **156**, 1234-1243

112. Leipelt, M., Warnecke, D., Zähringer, U., Ott, C., Müller, F., Hube, B., and Heinz, E. (2001) Glucosylceramide synthases, a gene family responsible for the biosynthesis of glucosphingolipids in animals, plants, and fungi. *J. Biol. Chem.* **276**, 33621-33629

113. Hartmann, D. O. (2014) Exploring ionic liquids′ unique stimuli to elucidate uncharacterised cellular and molecular mechanisms in filamentous fungi (Doctoral Dissertation). Instituto de Tecnologia Química e Biológica António Xavier - Universidade Nova de Lisboa

114. Markham, J. E., Li, J., Cahoon, E. B., and Jaworski, J. G. (2006) Separation and identification of major plant sphingolipid classes from leaves. *J. Biol. Chem.* **281**, 22684-22694

115. Chen, M., Markham, J. E., and Cahoon, E. B. (2012) Sphingolipid Δ8 unsaturation is important for glucosylceramide biosynthesis and low-temperature performance in *Arabidopsis*. *The Plant Journal* **69**, 769-781

116. Dickson, R. C. (2008) Thematic review series: sphingolipids. New insights into sphingolipid metabolism and function in budding yeast. *J. Lipid Res.* **49**, 909-921

117. Moreira, C. J. d. S. (2015) Deciphering novel targets for antifungal drugs: ionic liquids as triggers of alternative pathways for cell wall integrity in filamentous fungi (Master Dissertation). Universidade de Lisboa, Faculdade de Ciências

118. Spiegel, S., and Milstien, S. (2003) Sphingosine-1-phosphate: an enigmatic signalling lipid. *Nat. Rev. Mol. Cell Biol.* **4**, 397

119. Le Stunff, H., Galve-Roperh, I., Peterson, C., Milstien, S., and Spiegel, S. (2002) Sphingosine-1-phosphate phosphohydrolase in regulation of sphingolipid metabolism and apoptosis. *The Journal of cell biology* **158**, 1039-1049

120. Gunasekar, P., Borowitz, J., and Isom, G. (1998) Cyanide-induced generation of oxidative species: involvement of nitric oxide synthase and cyclooxygenase-2. *J. Pharmacol. Exp. Ther.* **285**, 236-241

121. Markham, P., Robson, G. D., Bainbridge, B. W., and Trinci, A. P. (1993) Choline: its role in the growth of filamentous fungi and the regulation of mycelial morphology. *FEMS Microbiol. Lett.* **104**, 287-300

122. Ryder, N. (1992) Terbinafine: mode of action and properties of the squalene epoxidase inhibition. *Br. J. Dermatol.* **126**, 2-7

123. Bailey, E. M., Krakovsky, D. J., and Rybak, M. J. (1990) The triazole antifungal agents: a review of itraconazole and fluconazole. *Pharmacotherapy* **10**, 146-153

124. Kamiński, D. M. (2014) Recent progress in the study of the interactions of amphotericin B with cholesterol and ergosterol in lipid environments. *Eur. Biophys. J.* **43**, 453-467

125. Newton, H. (2006) Clinical pharmacology of brain tumor chemotherapy: pyrimidine analogs. in *Handbook of brain tumor chemotherapy.* (Newton, H. ed.), Elsevier. pp 21-43